Journal of the Geological Society, London, Vol. **155,** 1998, pp. 957–973. Printed in Great Britain.

Integrated chronostratigraphy of the Vendian System of Siberia: implications for a global stratigraphy

SHANE M. PELECHATY

Department of Earth, Atmospheric, and Planetary Sciences, Massachusetts Institute of Technology, USA
Present address: Shell Research and Technical Services, Volmerlaan 8, 2280 AB, Rijswijk, The Netherlands
(e-mail: s.m.pelechaty@siep.shell.com)

Abstract: Integrated $\delta^{13}C$ chemostratigraphy and sequence stratigraphy are developed for a succession of Vendian strata (Nokhtuisk section) on the southern margin of the Siberian platform. The carbonates exhibit secular variations in $\delta^{13}C$ and at least three major depositional sequences that encompass the last *c.* 20 million years (<565–545 Ma) of Vendian time. Correlation of these events with key sections in eastern Siberia reveals the development of three cratonic sequences that partition the Vendian System of Siberia into high-resolution time slices (third-order sequences). The third-order events form a larger depositional sequence, which is correlated with greater confidence on a global-scale. With the aid of global chemostratigraphic constraints, the second-order sequence in Siberia is interpreted to represent the youngest of at least two sequences of eustatic origin that span the latest 60 million years of terminal Neoproterozoic time. Evidence for repeated glaciations in many basins at this time provides a plausible mechanism for the third-order cratonic sequences in Siberia. However, effects due to sea-floor spreading related to the break-up of the supercontinent Rodinia are invoked as the primary mechanism for the longer-term, second-order sea-level fluctuations.

Keywords: Vendian, Siberian Platform, chemostratigraphy, eustasy.

The Vendian System of Siberia is represented by a relatively thin (hundreds of metres thick) succession of mixed carbonaceous and siliciclastic rocks compared to other basins world-wide. However, the Siberian depositional record is well-preserved and covers most of the broad Siberian craton, and thus, provides a unique opportunity to investigate the significance of eustasy during Vendian and Cambrian times, a period noted for repeated glaciations (Saylor 1996; Kaufman *et al.* 1997) and global plate tectonic activity (Hoffman 1991). In Siberia, outcrops of Vendian strata are typically localized along river cuts. Their limited exposure, and the paucity of fossils in these rocks have necessitated crude lithostratigraphic methods for regional correlation. Consequently, the internal architecture and time partitioning of Vendian deposits in Siberia are poorly understood. Several recent stratigraphic studies, mainly in northern Siberia (i.e., Olenek uplift and Kharaulakh Mountains), have attempted to improve stratigraphic resolution by employing isotope carbon chemostratigraphy coupled with sequence stratigraphic methods for local and global correlation (Knoll *et al.* 1995*a*, *b*; Pelechaty *et al.* 1996*a*, *b*). This work has improved the understanding of Vendian stratigraphy in parts of Siberia, and has provided high-resolution temporal calibration that rivals, and in many cases exceeds, the stratigraphic resolution obtained in Phanerozoic basins.

This paper is divided into three sections and attempts to extend the chronostratigraphy established in the north across the eastern Siberian platform, and to other basins world-wide. The first section presents a detailed depositional and carbon isotopic history for a succession of well-exposed carbonates of the Nokhtuisk section in southern Siberia, located nearly 1000 km south of the Olenek uplift area. Then a high-resolution chronostratigraphic model for the Vendian System of eastern Siberia is presented based on regional correlation of nine stratigraphic sections. Finally, this chronostratigraphy is compared with key stratigraphic sections in a number of basins outside of Siberia in order to investigate the history and related mechanisms of global sea-level change during terminal Neoproterozoic time.

Geological setting

Terminal Neoproterozoic and Cambrian age rocks are superbly exposed along the Lena River, near the mouth of the Bolshoi Patom River and the village of Nokhtuisk in southern Siberia (Figs 1 and 2). These rocks are allochthonous and form the northern edge of the early Palaeozoic Predpatom orogenic belt (Nikulin 1970). North-verging thrusts of the Predpatom belt have tectonically juxtaposed Vendian age outer shelf and slope carbonates of the Nokhtuisk section on top of formerly up dip and coeval sabkha evaporites, which have been penetrated by hydrocarbon exploration wells located only tens of kilometres from the Nokhtuisk section (Grosman & Zhernovsky 1989).

The Nokhtuisk section is a composite of two closely spaced partial sections distributed across the Ura anticline (Fig. 2). The rocks on both limbs of the anticline dip steeply up to 80°. This study focuses on the Zherba and Tinnaya formations. Basal rocks of the Zherba Formation and older Neoproterozoic formations (Chencha Fm) are exposed on the northern limb of the anticline, and on the southern limb most of the Zherba Formation, and a complete section of the Tinnaya Formation, can be observed beneath younger deposits of the Nokhtuisk Formation. Exposure of the basal Zherba Formation contact at both sections allows correlation of the two sections and reconstruction of a nearly complete, 800 m thick composite. Only the middle 80 m of the Zherba

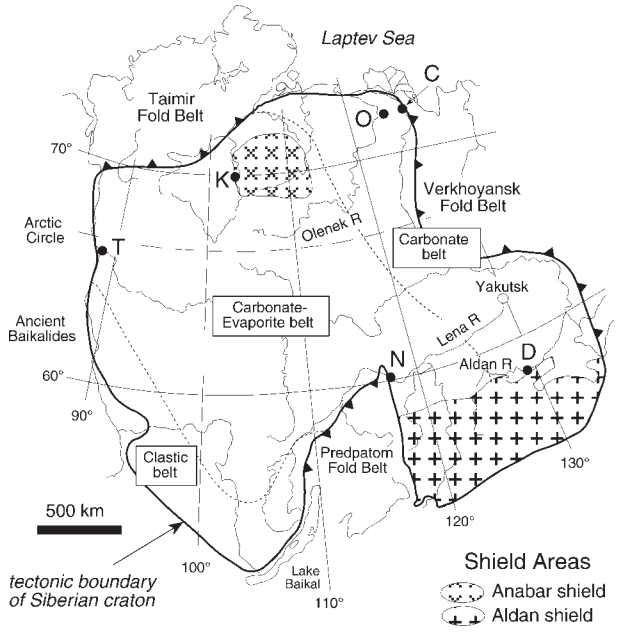

Fig. 1. Map showing the present-day position of the Siberian platform and location of key sections: Chekurov (C), Dvortsy (D), Koutikhan (K), Nokhtuisk (N), Olenek uplift (O; includes sections 1, 2, 3 and 4 in Fig. 9), and Turukhansk (T). Major rivers of eastern Siberia are shown, as well as the major facies provinces from Pelechaty *et al.* (1996*b*).

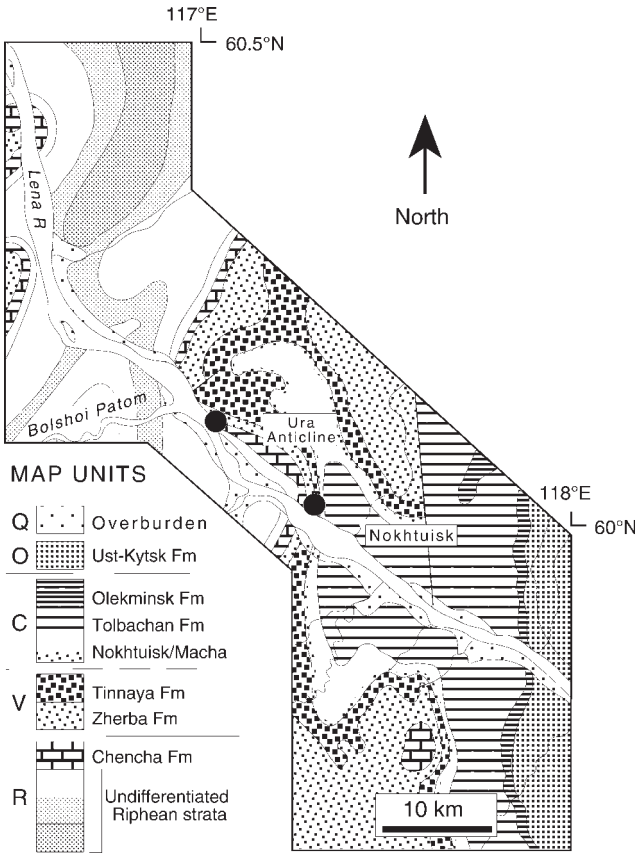

Fig. 2. Geological map of the Ura Anticline along the Lena River in southern Siberia. The Nokhtuisk section is a composite of two sections (solid circles) on the flanks of the anticline. Abbreviations: Q, Quaternary; O, Ordovician; C, Cambrian; V, Vendian; and R, Riphean.

Formation is covered at this location but stratigraphic information about this interval is available from exposures along the nearby Maly and Bolshoi Patom rivers (Khomentovsky 1986, 1990).

The Zherba Formation is 350 m thick and consists of a lower siliciclastic part and an upper carbonate part. The boundary between the Zherba and underlying Chencha formations is marked by interbedded carbonates and sandstones, and has been interpreted to signify conformity between the formations (Bobrov 1979; Khomentovsky 1990). However, regional stratigraphic studies by Shenfel and others (Shenfel & Yakshin 1975; Shenfel 1991) show this surface to be a regional angular unconformity, which they considered to mark the Riphean–Vendian boundary in southeastern Siberia. Field observations made during this field study indicate the development of a major unconformity at the base of the Zherba Formation in support of the interpretation of Shenfel and others.

The Tinnaya Formation consists of 350 m of carbonate conglomerates and minor sandstones. The formation is bounded by unconformities and is in turn overlain by mainly red sandstones, shales and minor carbonates of the Nokhtuisk Formation.

The ages of these formations are poorly constrained. The section contains acritarchs and stromatolites, but is barren of guide fossils suitable for biostratigraphic age determination (Kolosov 1975). Instead, calibration of these rocks is based on regional lithostratigraphic methods (Bobrov 1964; Kolosov 1975; Shenfel 1991), and reconnaissance carbon isotope chemostratigraphy (Sochava *et al.* 1996). The varicoloured rocks of the Nokhtuisk Formation have been correlated with Tommotian–Atdabanian age red beds that occur throughout southern Siberia, including the Petrosvet Formation along the Aldan River (Bobrov 1964; Kolosov 1975; Shenfel 1991). However, in the absence of biostratigraphic control, these interpretations have remained equivocal. Sochava *et al.* (1996) investigated the carbon isotope history of the upper Tinnaya, Nokhtuisk and younger formations in order to constrain time of deposition. On the basis of reconnaissance-level chemostratigraphic correlation with dated sections in Siberia, they placed the sub-Tommotian boundary approximately 200 m above the top of the Tinnaya carbonates in the Nokhtuisk Formation. Chemostratigraphic data presented in this study suggests that the lower 200 m of the Nokhtuisk Formation is correlative with the Nemakit–Daldyn Stage in the north, and that the Vendian–Cambrian boundary is positioned at the Tinnaya–Nokhtuisk contact.

Depositional facies

This section presents the sedimentology, stratigraphy and interpreted depositional facies for the Zherba and Tinnaya formations, and brief discussions of the bounding Chencha and Nokhtuisk formations. It forms the basis for the integrated sequence stratigraphic and chemostratigraphic framework that follows.

Chencha Formation

The Chencha Formation contains cross-bedded, grey oolitic limestones, dolomitic mudstones and buff stromatolitic

dolostones (Fig. 3), which are interpreted to represent a shallow-water platform composed of high-energy shoals and isolated, low-relief stromatolite reefs (Pelechaty 1997*a*). The upper 15 m of the formation contains mixed dolostones and sandstones. The dolostones show an upward colour change from buff to orange towards the Chencha–Zherba boundary. They gradationally overlie siliciclastic beds, which consist of green silty shales, cross-stratified glauconitic sandstones, and minor thin conglomerates. Interbeds of stromatolites, oolitic grainstones, teepee carbonates, intraformational breccias, and edgewise conglomerates are also present. The dolostones are cut by several erosion surfaces in the upper 2 m of the formation. The surfaces are coated with black chert and green glauconite, which are also found as clasts in overlying sandstones, and exhibit up to 50 cm of erosional relief associated with sand-filled fissures and small cavities, and local centimetre-size bladed crystals of anhydrite.

The erosion surfaces capping the dolostones at the top of the formation are interpreted to represent karst profiles associated with surface karren and shallow caverns. The discolouration of the dolostones may represent terra rossa (e.g. Estaban & Klappa 1983). Alternatively, the presence of chert and glauconite on these surfaces suggests that they are marine hardgrounds, however, these coatings may have formed during marine transgression of a karst landscape. In either case, a major unconformity is interpreted to mark the base of the Zherba Formation at this section.

Zherba Formation

The Zherba Formation is divided into four informal members, including in ascending stratigraphic order: sandstone, lower turbidite, bituminous carbonate, and upper turbidite (Fig. 3; Table 1). The formation is described in detail by Pelechaty (1997*a*).

The base of the formation is a succession of storm-influenced shelf deposits of the sandstone mbr and includes abundant trough (Fig. 4a) and hummocky cross-stratification, glauconite and intervals of outer shelf turbidites (Pelechaty 1997*a*). These deposits record an overall fining-upward trend, and above an 80 m interval of cover (Fig. 3), continues into the overlying lower turbidite mbr, which consists of centimetre-bedded sandstones, siltstones, and shales, and minor carbonates interpreted as outer shelf turbidites (Pelechaty 1997*a*). The transition between the sandstone and lower turbidite mbrs is gradational (Khomentovsky 1986, 1990). The top of the lower turbidite mbr arbitrarily includes the stratigraphically highest sandstones below the bituminous carbonate mbr, which represents an interval of interbedded black bituminous limestones, dolostones, and shaly dolostones. These deposits provide evidence of turbidite (laminated beds) and debris-flow (massive beds) sedimentation, and slumping indicative of a distal ramp environment. The bituminous carbonate mbr is sharply overlain by the upper turbidite mbr, a 66 m thick succession of siliciclastic and carbonate deposits. The lower 15 m of the upper turbidite mbr contains turbiditic sandstones, siltstones, and shales identical to those of the lower turbidite mbr, and overlying varicoloured carbonate turbidites consisting of interbedded grey and red limestones and buff dolostones (Fig. 4b). The upper 10 m of the upper turbidite mbr also contains trough cross-bedded quartzose conglomerates (Fig. 4c) and stromatolites, with the latter including two discrete horizons of black silicified bioherms interbedded with shelfal carbonates (Fig. 4d), and a thick biostromal bed capping the Zherba Formation (Fig. 4e, f). The capping biostrome shows exhumed symmetrical domes along a well-exposed bedding plane; this surface also reveals smooth shale-filled fissures that cut several centimetres into the bed. These fissures resemble karst dissolution cracks, and on the basis of their conspicuously smooth features, indicate that karstification occurred beneath a sediment mantle, interpreted to be the shales of the overlying Tinnaya Formation (Pelechaty 1997*a*).

Tinnaya Formation

The Tinnaya Formation is dominated by carbonate conglomerates (Bobrov 1979; Khomentovsky 1990; Shenfel 1991; Pelechaty 1997*a*), and is divided into four members, including in ascending order (Fig. 3; Table 2): quartz conglomerate, chip conglomerate (lower and upper members), raft conglomerate, and rudstone. The upper three members contain abundant carbonate conglomerates, and are described following the classification scheme of James & Stevens (1986) for similar deposits of the Cow Head Group in eastern Canada. Three major conglomerate types are recognized: chip conglomerates with centimetre-size equant clasts; plate conglomerates characterized by plate-like clasts centimetres thick and tens of centimetres in length; and raft conglomerates with metre-scale tabular blocks of bedded carbonate.

The quartz conglomerate mbr contains conglomerates, sandstones and shales (Pelechaty 1997*a*). The basal 0.7 m of the member consists of varicoloured (red, green, grey, and yellow) and crudely stratified shales that drape underlying stromatolitic and karstic relief (Fig. 4e). This bed is interpreted as a terra rossa mantle (e.g. Estaban & Klappa 1983) that formed during karstification of the underlying carbonates. The shales are overlain by unidirectionally trough cross-stratified conglomerates and sandstones, and shales interpreted to be both fluvial and shallow marine in origin (Pelechaty 1997*a*). The quartz conglomerate mbr is capped by stromatolitic and rippled dolostones, which are in turn sharply overlain by the carbonate conglomerates. The surface separating the dolostones and overlying conglomerates is interpreted as a significant marine flooding surface.

Description of the conglomerates. The chip conglomerates sharply overlie the quartz conglomerate mbr and grade upwards into the raft conglomerate mbr (Fig. 3). The chip conglomerates are divided into two members: the lower mbr consists of thin-bedded conglomerates, while the upper mbr includes relatively thick-bedded and coarser-grained conglomerates. The two members are separated by 10 m of quartz-bearing sediments, including thin-bedded, fine-grained sandstones, siltstones, and carbonate conglomerates with floating quartz sand, and clasts of carbonate mudstone, sandstone, and oolite (Fig. 3). The chip conglomerates throughout the rest of the section are typically barren of quartz sand. They are tabular-bedded (Fig. 4g, h), sharply bounded depositional units composed of centimetre-size clasts and minor plates that are arranged chaotically or locally with reverse grading (Fig. 5a, b). The deposits are clast-supported and contain carbonate mud matrices. Entire beds are typically composed of black bituminous limestones with some beds composed of dolostone clasts set in a limestone matrix, or vice versa. Clasts are commonly lime mudstones and dolomudstones with accessory

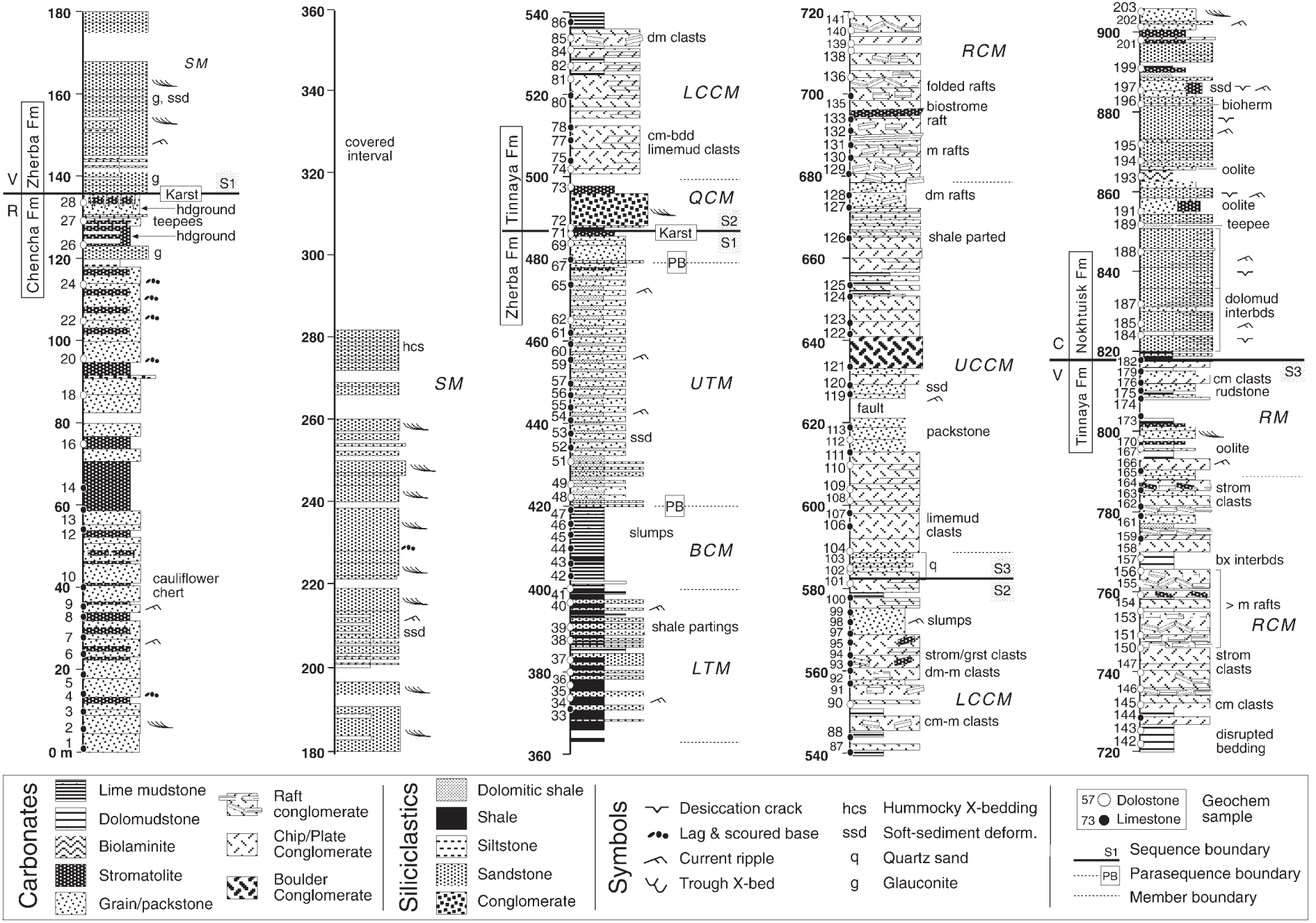

Fig. 3. Detailed stratigraphic column of the Nokhtuisk section. The lower 280 m of the section is from the north flank of the Ura Anticline, and the younger section crops out on the south flank.

Table 1. *Depositional units of the Zherba Formation*

Members	Constituents	Sedimentary structures	Interpretation	Vertical trends
Upper turbidite (UTM; 420–486 m)	Varicolored carbonates; sandstones, siltstones, and shales form lower 15 m and are also present in upper 6 m with carbonates	Lower 15 m like LTM; carbonates: cm-bedded, gray lime grainstones with ripples, planar lamination, soft-sediment deformation; buff dolostones (mudstones and stromatolites)	Siliciclastic and carbonaceous turbidites; shallow platform deposits	Carbonates increase up section; facies shallow up section
Bituminous carbonate (BCM; 400–420 m)	Thin-bedded black bituminous limestones, dolostones, shaly dolostones	Fining-up fine lamination; sharp-based massive beds, slump features, low-angle truncation, concretions	Distal ramp facies with turbidites and debris flows	No observed trends
Lower turbidite (LTM; 362–400 m)	Equal proportions of cm-bedded sandstones, siltstones, shales, and minor carbonates	Sandstones: massive, planar-laminated to rippled, individual beds fine upward; carbonates: black, bituminous limestones, dark gray dolostones	Distal turbidites	Carbonates increase up section
Sandstone (SM; 138–280 m)	Glauconitic sandstones, minor conglomerates, shales; tabular beds; shale partings; mudchips in sandstones	Sandstones: sharp-based, soft-sediment features, trough and hummocky cross-beds, planar lamination	Storm-influenced shelf deposits and outer shelf turbidites	Sediments fine- and deepen-upwards

lithoclasts of stromatolite (Fig. 5c), grainstone, and sandstone. Individual conglomerates are parted by carbonate mud, shale, or thicker intervals of bedded lime mudstones and dolomudstones (Fig. 4h). Minor rudstones and grainstones are found intercalated with the chip conglomerates, and show ripple cross-bedding and slump features.

The raft conglomerate mbr also contains chip conglomerates but is characterized by abundant raft conglomerates (Fig. 5d, 5e). Platy clasts and rafts are typically oriented subparallel to bedding and are set in finer chip-conglomeratic material. Rafts are composed of bedded lime mudstones and dolostones. Individual rafts tend to be folded (Fig. 5e), or broken along their lengths, forming 'trains' of smaller plates and rafts. Individual rafts may measure several metres in thickness and extend laterally beyond the limits of the outcrop. Such intervals of bedded limestones are interpreted as rafts on the basis of their bedding contacts, which tend to be truncated and show evidence of erosion and transport, and internal deformation, including small-scale folds, faults, and *in situ* breccia. Locally, large folded rafts can be traced laterally into chaotic plate and chip conglomerates (Fig. 5d). Other intervals of lime mudstones and dolomudstones appear to be *in situ* depositional units. The mudstones at the bases of these intervals onlap underlying sediments, while their upper contacts are either concordant with, or truncated by, carbonate conglomerates. In the upper part of the member, rafts are composed of bedded lime mudstones, grainstones, and stromatolitic dolostones.

The rudstone mbr gradationally overlies the raft conglomerate mbr to cap the Tinnaya Formation (Fig. 3). The rudstone mbr contains a variety of carbonates, including rudstones, grainstones, and packstones, fine chip conglomerates with centimetre-size clasts, stromatolites, and fetid dolomudstones. Grainstones and packstones are intraclastic to oolitic, and trough cross-stratified. The dolomudstones are present as finely laminated to massive beds containing floating chips of carbonate, which are thinly interstratified with beds and lenses of chip conglomerates. The very top of the member is represented by a 2 m thick chaotic chip conglomerate bed (Fig. 5f). It contains grey limestone clasts set in a dolomitic matrix. The clasts protrude above the top surface of the bed. The irregular surface of the conglomerate bed is draped by red sandstones of the Nokhtuisk Formation and does not show evidence of karst development.

Interpretation of the conglomerates. The conglomerates are interpreted to represent a spectrum of depositional processes indicative of a slope environment (e.g. Cook & Taylor 1977; James & Stevens 1986), including fall-out of suspended mud, slumping, debris flows, and turbidity currents. The Tinnaya conglomerates most likely represent sedimentation on a distally steepened ramp. The few shallow-water clasts found in the conglomerates suggest that the platform margin during this time was probably a series of ooid sand shoals and low-relief stromatolitic bioherms that prograded basinward into organic-rich muds on an unstable slope characterized by slumping.

In vertical succession, the Tinnaya carbonates reveal progressive degrees of deformation, which is interpreted to be related to increased transport on the slope (e.g. Cook & Taylor 1977; Cook & Mullins 1983). These facies include: (1) *in situ* bedded bituminous limestones that show no evidence of transport; (2) bedded limestones that show evidence for *in situ* deformation, including small-scale folding, brecciation, and faulting, interpreted to signal partial sliding; (3) internally folded bedded limestones that can be traced laterally into conglomerates; (4) large rafts of bedded limestones encased in conglomeratic material; and (5) chaotic platy and chip conglomerates. The slope is envisaged to have included an upper zone dominated by *in situ* carbonate mud deposits; a down dip zone of carbonate rafts that dislodged and were transported a limited distance down slope; and a distal zone dominated by platy and chip conglomerates, which formed as some rafts continued down slope and where broken up into finer conglomeratic material. This zonation is used to interpret the sequence stratigraphy for the Tinnaya Formation in the following section.

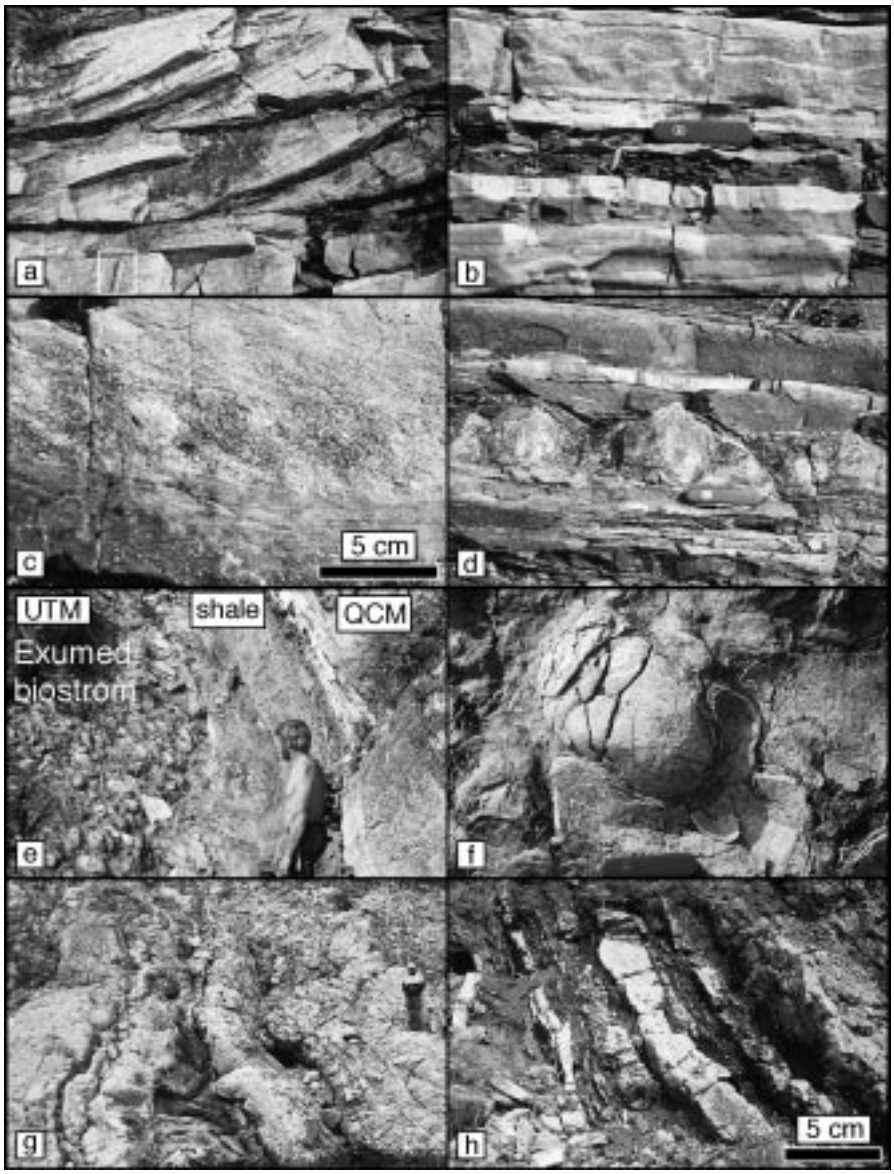

Fig. 4. Facies of the Zherba and Tinnaya formations. Zherba Formation: (a) trough cross-bedded shelf sandstones (SM); hammer for scale; (b) rippled calcareous turbidites (UTM); pen knife for scale; (c) trough cross-bedded quartzose conglomerate (UTM); (d) silicified bioherms interbedded with sandstones (UTM); pen knife for scale; (e) upper surface of a stromatolitic dolostone bed (UTM), overlain by deposits of the Tinnaya Formation; and (f) exhumed stromatolite dome with shale-filled karst fissures at the top of the Zherba Formation; pen knife for scale. Tinnaya Formation: (g) thick-bedded chip and raft conglomerates; and (h) thin-bedded chip conglomerates separated by recessive, black shaly limestone.

The platy and chip conglomerates are probably debris flows. Field observations demonstrate that the ancient flows had matrix strength and buoyancy (e.g. Cook & Taylor 1977; Cook & Mullins 1983; Hiscott & James 1984); these include: (1) beds with sharp, non-erosive bases; (2) chaotic sorting and subparallel arrangement of tabular clasts; and (3) outsized clasts at the top of beds that protrude upwards above the surrounding bed surface.

The stratified and cross-bedded conglomerates, rudstones, and grainstones at the top of the Tinnaya Formation are interpreted to be turbidites. They contain abundant clasts of shallow-water affinity and suggest that turbidity currents initiated on the shallow outer platform by spontaneous flow initiation. Turbidity currents may have been generated during storms and moved basinward as sediment-laden, gravity-induced currents.

Nokhtuisk Formation

The studied basal 80 m of the Nokhtuisk Formation is dominated by clastic red beds, including centimetre-scale interbedded sandstones, siltstones, and shales, plus minor dolostones (Fig. 5g). The sandstones are planar to ripple cross-laminated and grade upward into siltstones and shales, which are typically laminated and exhibit well-developed polygonal desiccation cracks (Fig. 5h). The dolostones consist of oolitic grainstones, massive mudstones, teepee beds, and domal stromatolites. Some grainstones contain clastic gypsum. Dolostones also form conglomerates and clasts at the bases of sandstones.

The basal Nokhtuisk Formation contains a succession of siliciclastic and carbonate deposits that reflect deposition in very shallow-water with evidence of evaporative conditions and subaerial exposure. Such conditions are common on coastal mud flats (e.g. Klein 1977; Weimer *et al.* 1982).

Sequence stratigraphic analysis

The Zherba and Tinnaya formations are interpreted to display at least three depositional sequences (Fig. 3), which are recognized by the vertical distribution of unconformities, depositional facies, and siliciclastic detritus. The Zherba Formation

Table 2. *Depositional units of the Tinnaya Formation*

Members	Constituents	Sedimentary structures	Interpretation	Upward trends
Rudstone (RM; 790–820 m)	Rudstones, grainstones, packstones, chip conglomerates, stromatolites and fetid dolomudstones	Rudstones etc: intraclastic to oolitic, trough cross-beds; Dolo-mudstones: finely laminated to massive with conglomerate lenses	Outer platform traction deposits	NA
Raft conglomerate (RCM; 670–790 m)	Carbonate conglomerates; meter-scale rafts	Folded rafts; Sharply-bounded beds; subparallel oriented clasts	Inner slope conglomerates	Proportion of carbonates increase and facies shallow upwards
Upper chip conglomerate (UCCM; 582–670 m)	Thick-bedded carbonate conglomerates	NA	Outer slope conglomerates	NA
Lower chip conglomerate (LCCM; 500–582 m)	Thin-bedded carbonate conglomerates; minor lime mudstones, dolomudstones, grainstones and shales	Conglomerates: chip, minor platey clasts and rafts, chaotic, local reverse grading	Outer slope conglomerates	Proportion of rafts, shallow clasts, and *in situ* mudstones increase upwards
Quartz conglomerate (QCM; 486–500 m)	Lower 0.7 m varicolored shales; conglomerates, sandstones, shales and minor dolostones	Conglomerates, sandstones: trough cross-beds; Dolostones: grainstones and stromatolites	Fluvial to shallow marine; Basal shale is interpreted as a terra rossa soil	Sediments fine and deepen upwards

is bounded by significant erosion surfaces and is interpreted to represent a single, unconformity-bounded depositional sequence (Sequence 1) comprised of a relatively conformable succession of strata. Stratigraphic sections to the south described by Khomentovsky (1986) support this interpretation; they reveal a fining-upward trend across the equivalent covered interval at the Nokhtuisk section. The sequence is divided into transgressive and highstand systems tracts. The transgressive part of the sequence is represented by the sandstone, lower turbidite and bituminous carbonate mbrs, and together these members record an overall deepening of facies and reduction of siliciclastic detritus up section. The bituminous limestones of the bituminous carbonate mbr may represent an interval of maximum flooding and conditions of starved siliciclastic sedimentation in response to a maximum landward shift of coastal facies. The highstand systems tract is represented by the upper turbidite mbr, which records an overall shallowing of sea-level. The upper turbidite mbr exhibits at least two distinct siliciclastic-to-carbonate parasequences, and together, they show a pattern of thinning up section, which may indicate terminal highstand conditions. Complete shoaling to sea-level and exposure of the shelf is represented by the palaeokarst profile at the top of the Zherba Formation.

The Tinnaya Formation is interpreted to include at least two additional depositional sequences (Fig. 3). Evidence for changes in relative sea-level includes vertical changes in conglomerate type and associated facies, clast composition, and partitioning of siliciclastic detritus. Sequence 2 is interpreted to include the quartz conglomerate mbr and lower chip conglomerate mbr up to the base of the quartz-bearing deposits at the top of the lower chip conglomerate mbr. The basal quartz conglomerates are interpreted as transgressive deposits. They are sharply overlain by transgressive to highstand conglomerates along a significant marine flooding surface, which marks a pronounced change from shallow-water to deep-water conditions. The carbonate conglomerates are considered to record a gradual fall in relative sea-level from the base to the top of the lower chip conglomerate mbr. This sea-level change is represented by an upward increase in the proportion of shallow-water lithoclasts in the conglomerates, and an upward increase in the proportion of *in situ* bedded mudstones.

Sequence 3 is represented by the upper chip conglomerate, raft conglomerate and rudstone mbrs. The interbedded quartzose conglomerates, sandstones, and siltstones mark the base of Sequence 3 and are interpreted to represent a drop in relative sea level and a basinward influx of siliciclastic sediment onto the slope (e.g. Vail *et al.* 1984). Above this level, a return to relatively deep-water conditions is marked by a pronounced change in clast composition in the conglomerates, from shallow-water lithologies at the top of Sequence 2 to deep-water mudstone clasts above the quartz-bearing carbonates. This transition is interpreted to reflect an abrupt proximal to distal shift in slope deposition. The conglomerates of Sequence 3 also reveal an upward-shoaling trend on the basis of similar features displayed by the conglomerates of Sequence 2, plus an upward increase in the abundance of large rafts, *in situ* folded bedded carbonates, traction deposits (i.e. rudstones, grainstones) and stromatolites. The sharp contact between the Tinnaya conglomerates and overlying Nokhtuisk tidal flat deposits is interpreted to represent a major sequence boundary. The absence of subaerial exposure indicators along the top of the Tinnaya carbonates suggests that the Nokhtuisk sediments were deposited over the outer Tinnaya platform during a major basinward shift in facies. The tidal flat clastics of the Nokhtuisk Formation are interpreted to mark the base of a separate depositional sequence.

Isotopic data and results

The $\delta^{13}C$ and $\delta^{18}O$ profiles for the Nokhtuisk section are based on analyses of over 150 stratigraphically closely spaced carbonates from this study (Table 3), and an additional 27 pairs of samples by Sochava *et al.* (1996; Fig. 6). They also report accompanying elemental (Fe, Mn and Sr) compositions, which are used to interpret the diagenetic grade of the sampled carbonates. Selection of carbonate samples follows methods described by Pelechaty *et al.* (1996*a*). In brief, individual

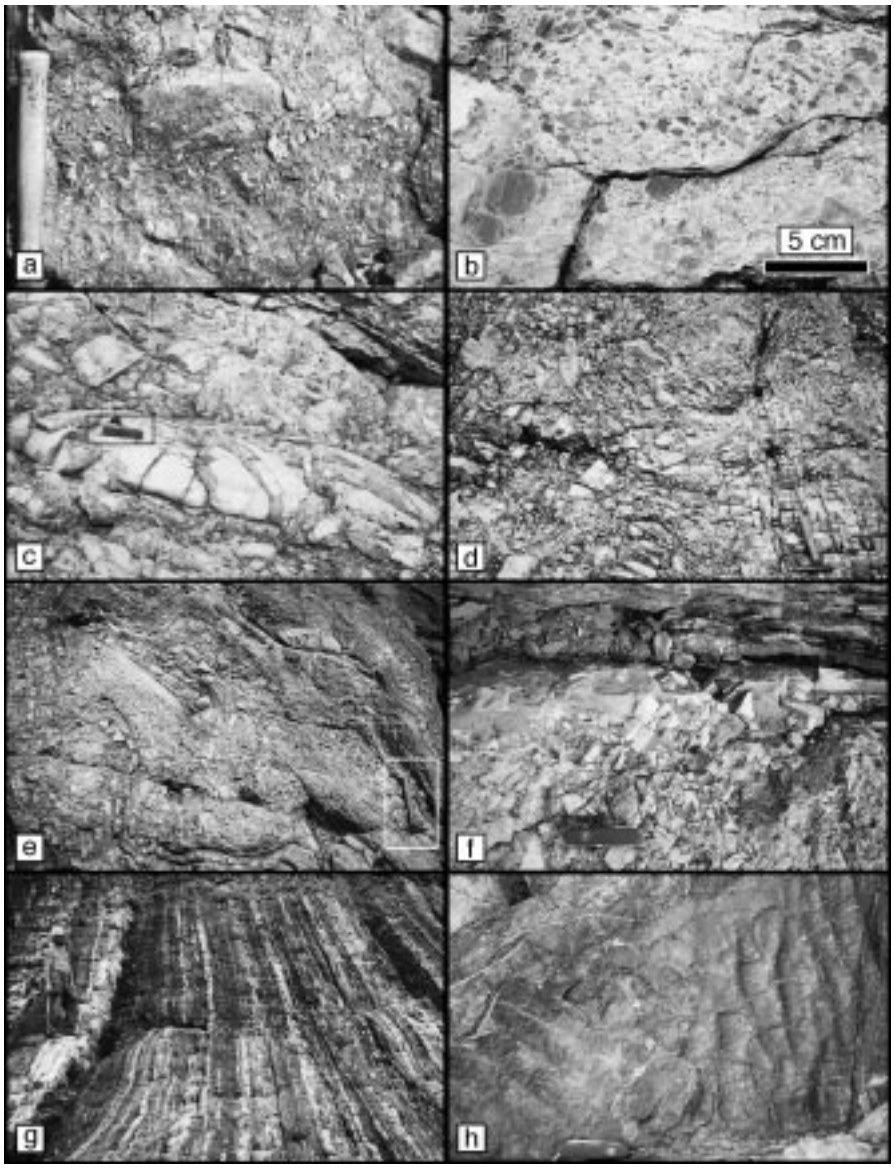

Fig. 5. Facies of the Tinnaya and Nokhtuisk formations. Tinnaya Formation: (a) and (b) chip conglomerate beds; (c) raft conglomerate with stromatolite blocks; pen knife sits on a stromatolite clast; (d) raft conglomerate with raft and chip fragments; hammer for scale rests on a raft; (e) thick, folded raft conglomerate beds; hammer for scale; and (f) chip conglomerate capping the Tinnaya Formation—note the clasts that protrude from the top of the bed are draped by sandstones of the Nokhtuisk Formation; pen knife for scale. Nokhtuisk Formation: (g) red beds: interbedded sandstones (massive beds), siltstones and shales (recessive beds); and (h) bedding surface of sandstone showing ripples and mudcracks; pen knife for scale.

depositional components with minimal signs of recrystallization were sampled, including micritic carbonate from massive and laminated detrital sediment, and micritic clasts and matrix material from conglomerates. The isotopic composition of these samples was analysed at the University of Michigan using standard laboratory procedures, which are summarized by Saltzman *et al.* (1995).

Oxygen isotope composition

The carbonates of the Nokhtuisk section reveal extreme variability in $\delta^{18}O$, ranging between 0 and -20‰ PDB (Fig. 6). Notably, these data separate into two distinct isotopic groups according to lithology. In general, the limestones are depleted by varying amounts relative to the dolostones in the section. This pattern has also been reported from this section by Sochava *et al.* (1996) and Pokrovsky & Gertsev (1993). The Chencha Formation is characterized by values between -8.8‰ and -3.4‰, with the limestones being more depleted than the dolostones. Higher in the section, the upper Zherba Formation is characterized by dolostones with values between approximately 0 and -6‰, and limestones between -3.6 and -9.4‰; the limestones become less depleted relative to the dolostones towards the top of the formation. The Tinnaya Formation reveals the most pronounced separation of isotopes by lithology. The limestones have values between -15 and -20‰. They are depleted by as much as 10‰ in ^{18}O relative to interbedded dolostones in the upper part of the Tinnaya Formation and lower Nokhtuisk Formation, which all range generally between -5 and 0‰. A few dolostones, however, exhibit values similar to the limestones near the 600 m level in the Tinnaya Formation.

Carbon isotope composition

The $\delta^{13}C$ values from both the limestones and dolostones, which include a spectrum of depositional facies, define a single, smoothly varying curve through most of the section with only a few outlying data points (Fig. 6). At the base of the profile, the carbonates of the Chencha Formation exhibit a slight rise in $\delta^{13}C$ values from -9 to -4.6‰ up section. This pattern is also reported by Pokrovsky & Gertsev (1993). The upper

Table 3. *Summary of stable isotopic and petrographic analyses (see Fig. 3 for sample location)*

No.	Height	$\delta^{13}C$	$\delta^{18}O$	Sample
Chencha Formation				
1	1.0	−9.0	−8.6	L slt M*
2	5.5	−9.3	−8.6	L slt M
3	10.0	−8.9	−8.4	L slt M
4	14.5	−8.3	−8.2	L md S
5	19.0	−8.6	−8.8	L md M
6	24.0	−8.4	−7.0	L md M
7	28.5	−8.5	−8.0	L md M
8	33.0	−8.4	−8.0	L md M
9	35.5	−8.8	−7.7	L md M
10	40.0	−10.4	−7.7	L bm M
12	54.5	−8.8	−7.9	L bm M
13	59.0	−7.9	−7.1	L bm M
14	64.6	−8.6	−7.6	L bm O
16	75.0	−7.4	−3.6	D bm M
18	87.0	−7.9	−5.1	D bm M
20	96.0	−7.1	−5.0	D md M
22	105.0	−7.6	−5.2	D md M
24	114.0	−7.0	−5.0	D md M
26	123.0	−6.2	−5.0	D md S
27	129.5	−5.5	−3.4	D md M
28	134.0	−4.6	−4.6	D md M
Zherba Formation (Sequence 1)				
33	371.5	−8.6	−7.3	L md M
34	374.5	−13.3	−2.1	D md M
35	377.5	−11.0	−2.0	D md N
36	380.5	−15.4	−2.7	D md S
37	383.5	−15.5	−1.7	D md M
38	388.0	−15.8	−2.4	D md M
39	391.0	−19.5	−2.1	D md S
40	397.0	−20.1	−0.2	D gs M
41	400.0	−16.9	−6.0	D gs C
42	403.0	−9.7	−5.8	L gs C
43	406.5	−4.2	−9.4	L gs C
44	410.0	−3.2	−9.2	L gs C
45	413.0	−1.8	−8.4	L gs M
46	416.0	−2.7	−7.1	L gs N
47	419.0	−1.0	−8.0	L gs N
48	422.5	−6.3	−2.3	D gs C
49	425.5	−2.1	−1.2	D gs N
51	431.5	−2.9	−1.4	D gs N
52	434.5	−2.7	−4.7	L gs C
53	437.5	−4.8	5.4	L gs N
54	441.0	−1.8	−4.6	L gs N
55	444.0	−1.3	−3.6	L gs W
56	447.0	−1.4	−4.4	L gs C
57	450.0	−1.5	−4.7	L gs C
59	456.5	−2.2	−4.5	L gs C
60	459.0	−1.1	−4.4	L gs M
61	462.0	0.3	−4.2	L gs C
62	465.0	0.4	−1.6	D gs M
65	474.0	2.2	−4.7	L gs M
67	480.5	1.8	−5.9	L gs M
69	483.5	1.3	−1.9	D gs M
71	486.5	2.1	−3.1	D st M
72	488.0	1.4	−1.8	D gs C
Tinnaya Formation (Sequence 2)				
73	498.5	0.9	−3.2	D md M
74	502.5	−0.4	−6.7	D md M
75	505.0	−2.6	−19.8	L bx M
77	509.5	−2.4	−19.4	L bx M
78	512.5	−2.9	−18.6	L bx M
80	520.5	−2.9	−19.8	L gs
81	524.5	−1.6	−17.5	L bx M
82	527.5	−3.2	−17.2	L bx M
84	531.5	−1.9	−16.5	L bx M
85	534.5	−0.2	−17.9	L gs W
86	537.5	−0.9	−19.1	L gs M
87	540.5	0.3	−14.0	L bio M
88	544.0	−0.2	−19.3	L gs M
90	552.5	−0.5	−9.4	D gs M
91	556.5	−1.2	−18.5	L st M
92	560.0	−1.2	−17.3	L st M
93	561.5	−1.1	−18.4	L slt M
94	564.0	−0.9	−20.0	L slt M
95	567.0	−2.3	−19.3	L bio M
97	569.0	−4.5	−19.8	L bslt M
98	572.0	−4.8	−19.9	L bm M
99	574.5	−3.9	−19.5	L bm M
100	578.0	−2.0	−19.0	L bm M
101	581.0	−1.8	−15.4	D bm M
Tinnaya Formation (Sequence 3)				
102	584.0	−2.9	−16.1	D bm M
103	585.0	−4.2	−17.0	L bm M
104	589.0	−6.5	−16.6	D gs S
106	595.0	−2.9	−19.4	L bm M
107	598.0	−3.8	−19.1	L bm M
108	601.0	−2.7	−16.5	D bm M
109	604.0	−4.2	−17.7	D bm M
110	610.0	−4.1	−15.4	D md M
111	613.0	−6.1	−17.3	L md M
112	616.0	−6.3	−16.8	D bx S
113	619.0	−7.9	−17.3	L md M
119	627.0	−7.3	−18.4	L md M
120	629.0	−8.9	−17.5	L md S
121	633.5	−6.0	−19.5	L md M
122	641.5	−4.7	−19.7	L md M
123	644.5	−2.9	−15.9	L md M
124	651.0	−5.9	−18.7	L md M
125	653.5	−5.2	−17.0	L md M
126	665.0	−6.3	−19.3	L md M
127	672.5	−6.0	−19.5	L md M
128	675.5	−5.6	−17.2	L md M
129	680.0	−7.8	−19.5	L md M
130	684.5	−4.3	−19.7	L md M
131	687.5	−4.4	−17.3	L md M
132	691.0	−3.6	−17.7	L md M
133	694.0	−4.7	−15.2	L md M
135	700.0	−4.9	−15.7	L md M
136	704.0	−4.5	−1.5	D md M
138	710.5	−5.0	−0.3	D md M
139	712.0	−6.0	−1.3	D md M
Tinnaya Formation (Sequence 3) continued.				
140	715.0	−5.5	−1.0	D md M
141	719.0	−9.3	−1.0	D gs B
142	722.0	−6.8	−1.2	D gs N
143	725.0	−6.5	−0.5	D gs S
144	728.5	−6.0	−17.4	L gs B
145	731.5	−4.1	−0.9	D gs C
146	736.0	−3.3	−1.1	D gs W
147	740.0	−3.3	−1.0	D gs C
150	746.0	−3.1	−1.9	D gs B
151	749.5	−3.8	−4.6	D gs B
153	755.5	−3.1	−2.4	D gs C
154	759.5	−3.5	−1.5	D gs S
155	762.5	−4.2	−3.8	D gs C
156	765.5	−7.4	−2.9	D gs C
157	768.5	−8.0	−2.6	D gs S
158	771.0	−7.0	−2.3	D gs C
159	773.5	−3.8	−15.0	L gs C
161	779.0	−3.3	−18.4	L gs S
162	781.5	−3.2	−15.7	L gs C
163	785.5	−3.9	−18.1	L gs C
164	788.5	−2.4	−3.0	D gs S
165	790.5	−2.6	−14.9	L gs C
166	793.5	−2.6	−3.0	D gs C
167	795.5	−2.8	−2.6	D md N
170	798.5	−2.3	−3.6	D md N
173	803.5	−3.9	−17.0	L md M
174	808.5	−3.1	−20.4	L md M
175	810.0	−2.7	−19.2	L gs C
176	812.0	−3.3	−20.5	L md M
179	815.0	−2.7	−20.1	L md S
Nokhtuisk Formation (Sequence 4)				
182	818.5	−2.3	−20.2	L md M
184	824.0	−4.4	−4.1	D md M
185	827.0	−3.7	−2.7	D md M
187	832.0	−4.2	−3.4	D md M
188	845.0	−1.3	−3.7	D gs C
189	852.0	−0.8	−3.8	D gs C
191	855.5	0.0	−4.0	D gs C
193	864.0	0.6	−3.2	D gs W
194	868.0	0.0	−3.4	D gs W
195	872.0	0.6	−3.4	D gs W
196	882.5	−1.6	−3.8	D gs C
197	885.5	−0.5	−4.0	D gs C
199	891.0	−2.3	−3.1	D st M
201	898.5	−0.3	−4.4	D st M
202	901.5	−0.2	−4.8	D st M
203	905.0	1.3	−6.0	D st M

Lithology: L, limestone; D, dolostone. Sediment type: gs, grainstone; slt, siltstone; md, mudstone; bm, bituminous mudstone; st, stromatolite; bio, biolaminite; bx, breccia. Allochem: M, micrite, O, organic-rich micrite; N, neomorphic spar; C, micritic clast; B, baroque spar; S, spar fill; W, whole rock.

Zherba Formation, however, reveals greater variability in $\delta^{13}C$. The lower turbidite mbr between 370 and 400 m contains dolostones with very light values between −20 and −15‰. Above this interval in the Zherba Formation, interbedded limestones and dolostones have heavier values, which define a high-frequency curve superposed on an overall increasing positive trend from −4.2 to +2.2‰ up section. The entire Tinnaya and lower Nokhtuisk formations reveal a relatively tight and well-defined curve, which forms a first-order negative anomaly. The lower 150 m of the Tinnaya Formation is

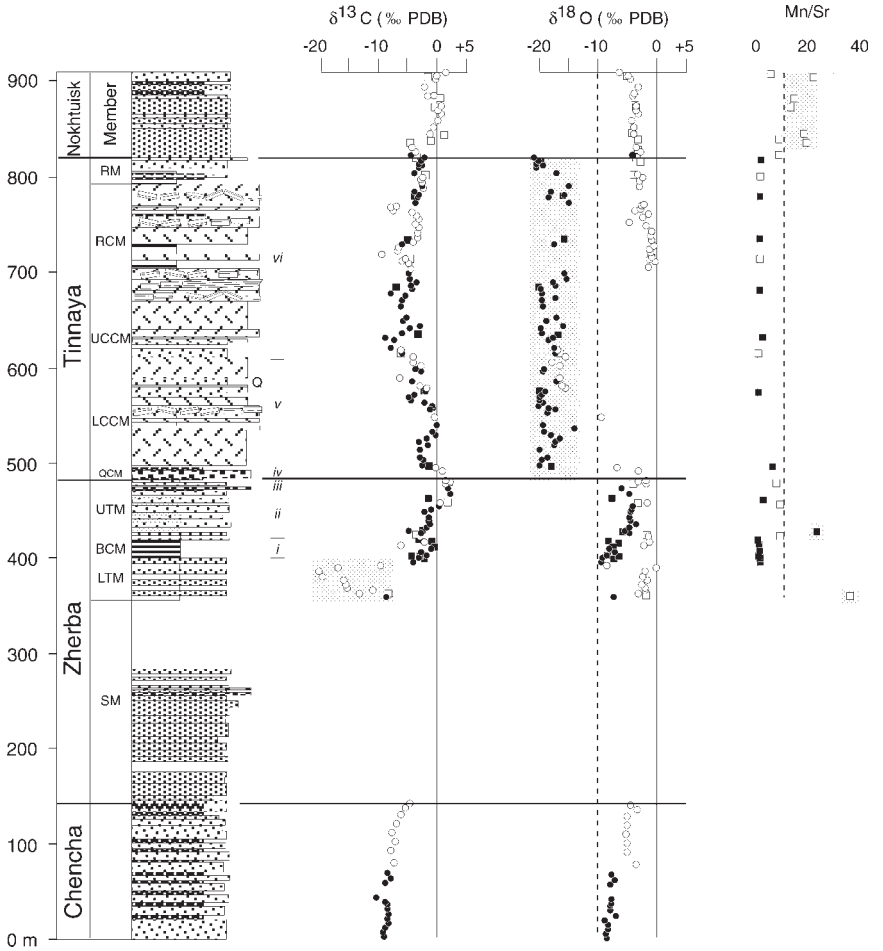

Fig. 6. Generalized stratigraphic column of the Nokhtuisk section with accompanying isotopic and Mn/Sr profiles. Symbols: solid circles (limestone) and open circles (dolostones) are results of this study; solid squares (limestone) and open squares (dolostones) are results of Sochava *et al.* (1996). Sample locations from this study are shown in Fig. 3. Units designated by Bobrov (1964) are shown as Roman numerals. Shaded areas indicate altered samples according to $\delta^{18}O < -10‰$ and Mn/Sr>10 and other factors (see text).

characterized by decreasing $\delta^{13}C$ values from +1 to −9‰ up section, followed by an overall increase in values to +1.3‰ in the lower Nokhtuisk Formation. High-frequency, <5‰ shifts are superposed on this large magnitude negative excursion.

Mn/Sr

Although elemental geochemistry of the carbonates was not carried out during this study, Mn/Sr was measured from selected samples by Sochava *et al.* (1996) and provide added information on the diagenetic history of these carbonates. Data of Sochava *et al.* (1996) cover an interval from the upper Zherba Formation to several hundreds of metres above the Tinnaya–Nokhtuisk formational contact (Fig. 6). High Mn/Sr of 38 occurs at the base of the lower turbidite mbr in association with carbonates strongly depleted in $\delta^{13}C$. The bituminous carbonate mbr has Mn/Sr<2; the upper turbidite mbr records Mn/Sr<10; and the Tinnaya Formation reveals Mn/Sr<2. The lower 100 metres of the Nokhtuisk Formation is characterized by Mn/Sr<22 but above this level (not shown in Fig. 6) the upper Nokhtuisk Formation shows Mn/Sr<2 (Sochava *et al.* 1996).

Discussion of isotopic trends

The elemental and isotopic abundances from the carbonates of the Nokhtuisk section vary widely. Many authors have used Mn/Sr>10 and $\delta^{18}O < -10‰$ to identify 'altered' carbonates (Kaufman *et al.* 1991; Knoll *et al.* 1995*a*; Kaufman & Knoll 1995; Pelechaty *et al.* 1996*a*). Three intervals in the section are highlighted as being altered with respect to their $\delta^{18}O$ and Mn/Sr systems (Fig. 6): (1) carbonates in the upper Zherba Formation with high Mn/Sr and strongly depleted $\delta^{13}C$ values; (2) limestones and a few dolostones of the Tinnaya Formation with strongly depleted $\delta^{18}O$; and (3) dolostones in the lower Nokhtuisk Formation with high Mn/Sr. These three intervals will now be discussed in turn.

(1) The carbonates of the lower turbidite mbr in the Zherba Formation are indicated as altered (Fig. 6). The single Mn/Sr sample at the base of the lower turbidite mbr records the highest Mn/Sr in the section, and is associated with extremely light $\delta^{13}C$ values between −20 and −15‰. The section is considered to represent obvious diagenetic alteration and resetting of ^{13}C. Such values are typical of carbonates that have undergone diagenesis in association with oxidation of sedimentary organic matter (Anderson & Arthur 1983; Claypool & Threlkeld 1983; Kocurko 1986). The association of very light dolomites and organic-rich sediments suggests that the carbonates of the lower turbidite mbr were dolomitized early during oxidation of interstitial sedimentary organic matter (e.g. Pisciotto & Mahoney 1981). Although the overlying bituminous carbonate mbr also contains organic-rich carbonates, the sandstones and shales present in the lower turbidite mbr probably facilitated the migration of diagenetic fluids through this section. Thus, the $\delta^{13}C$ values through the lower turbidite mbr are interpreted not to be stratigraphically significant.

(2) The Tinnaya Formation reveals strongly depleted $\delta^{18}O$ but low Mn/Sr (Fig. 6). This is consistent with observations of recrystallization of carbonates, also reported by Sochava *et al.* (1996), and a slope depositional setting for the carbonates for stratigraphically restricted hydrothermal fluid flow during burial diagenesis. Sochava *et al.* (1996) also suggested that the depleted limestones may in part record meteoric alteration, which may also cause isotopic depletion of carbonates (Anderson & Arthur 1983). Although the origin of meteoric fluids in the basin is difficult to determine with existing data, such fluids may have flushed through the Tinnaya aquifer during early Palaeozoic mountain building and formation of the Predpatom orogenic belt.

The enriched $\delta^{18}O$ composition of the dolostones in the Tinnaya Formation records a different diagenetic history. The presence of dolomitic clasts and lime matrix in some conglomerates suggests that dolomitization occurred early, at least prior to transport of clasts into the basin. The relatively limited susceptibility of dolostones to meteoric corrosion (e.g. Choquette & James 1988), and low relative permeability, may have been important in isolating the dolostones during burial diagenesis. This is interpreted to have affected the interbedded limestones in the formation. However, some dolostones were obviously affected by burial fluids, as suggested by the depleted dolostones in the middle of the formation. They occur in close proximity of a sequence boundary and with sandstones that were likely permeable and exposed the interbedded dolostones to diagenesis. The enriched dolostones may record early, near-surface diagenesis. The presence of coeval evaporites up dip of the Nokhtuisk section (Grosman & Zhernovsky 1989; Kuznetsov & Suchy 1992) may indicate sabkha-style dolomitization. This diagenetic interpretation is consistent with the position of the dolostones near unconformity surfaces in the section, and their association with relatively shallow-water facies. Furthermore, the presence of evaporites in the overlying Nokhtuisk Formation sandstones, and the regional climatic setting of a rain shadow along the Baykalide mountains for this region (Pelechaty *et al.* 1996*b*) is consistent with a sabkha-related diagenetic history for the enriched dolostones.

Although the Tinnaya carbonates have undergone several diagenetic episodes, as suggested by the $\delta^{18}O$ data, the $\delta^{13}C$ values through the formation do not correlate with the $\delta^{18}O$ record, and suggest that the carbon isotopic composition of the carbonates may not have been affected by diagenesis. Furthermore, the negative $\delta^{13}C$ trend does not correlate with the distribution of limestones and dolostones, or depositional facies in the section. The Tinnaya excursion displays depleted values to $-9‰$, which may in part reflect diagenetic resetting as suggested for the highly depleted $\delta^{13}C$ values in the lower turbidite mbr; however, similar magnitude shifts to the Tinnaya excursion are documented in northwest Canada (Narbonne *et al.* 1994), in the western Anabar region of northern Siberia (Knoll *et al.* 1995*b*; Kaufman *et al.* 1996), and in Mongolia (Brasier *et al.* 1996) of slightly lower magnitude that are interpreted to be secular in origin. It is suggested that the $\delta^{13}C$ profile through the Tinnaya Formation represents secular variation.

(3) Some dolostones in the lower part of the Nokhtuisk Formation also show evidence of alteration with high Mn/Sr between 10 and 22. These carbonates are interbedded with dolostones with low Mn/Sr, but both sets of carbonates reveal similar $\delta^{13}C$ compositions. Above this interval, nearly 500 m of mainly limestones exhibit Mn/Sr<2 (Sochava *et al.* 1996). The localization of high Mn/Sr at the base of the Nokhtuisk Formation indicates that the carbonates were altered by fluids that passed along the unconformity in sandstone aquifers. Similar diagenetic-stratigraphic relationships have been made at the Chekurov anticline section in the Kharaulakh Mountains (Pelechaty *et al.* 1996*a*).

Despite the presence of altered carbonates in the section, the smoothly varying $\delta^{13}C$ trend suggests that the measured isotopic compositions can be used to define secular trends in $\delta^{13}C$ throughout most of the section.

Stratigraphic significance of the Nokhtuisk $\delta^{13}C$ profile

The $\delta^{13}C$ profile through the Zherba and Tinnaya formations displays patterns that are consistent with the Vendian carbon isotopic record observed elsewhere in Siberia and world-wide. The Nokhtuisk profile is interpreted to record secular variation with allowances for effects due to basin subsidence and stratigraphic hiatuses with only localized diagenetic overprint. The temporal significance of the carbon isotope profile is also compatible with stratigraphic constraints. Notably, red beds of the Nokhtuisk Formation are considered to be early Cambrian in age on the basis of their lithological similarity with the dated Petrosvet Formation in southeastern Siberia (Bobrov 1964; Kolosov 1975; Magaritz *et al.* 1986; Shenfel 1991). In addition, Sochava *et al.* (1996) recognized similar broad $\delta^{13}C$ patterns between the Nokhtuisk, composite Aldan–Lena, and Kotuikan River sections using reconnaissance data to support an early Cambrian age for the Nokhtuisk Formation.

The $\delta^{13}C$ profile of the Zherba and Tinnaya formations is divided into at least four major isotopic events of interpreted Vendian age. These events include, in ascending chemostratigraphic order (Fig. 7): (1) a negative excursion (N2); (2) a positive excursion (P); (3) an intermediate isotopic interval (I); and (4) a prominent negative isotopic shift (N1). The Tinnaya negative shift (N1) is compatible with a Vendian age; world-wide, carbonates just beneath the Vendian-Cambrian boundary (base of Nemakit–Daldyn Stage) are associated with similar negative shifts (Kaufman & Knoll 1995). On the basis of this observation, the base of the Nemakit–Daldyn Stage (Vendian–Cambrian boundary) is positioned at the Tinnaya–Nokhtuisk contact, approximately 200 m below the sub-Tommotian boundary defined by Sochova *et al.* (1996).

The base of the Vendian section is placed at the unconformity separating the Chencha and Zherba formations. The $\delta^{13}C$ composition of the Chencha Formation carbonates is lighter than other known Riphean carbonates of Siberia (Pokrovsky & Missarzhevsky 1993; Knoll *et al.* 1995*c*), but in light of limited data from this interval, their age cannot be confirmed at present.

Further up section, the N1 anomaly is the most distinctive feature of the isotopic profile. It shows a large magnitude excursion up to $-9‰$ over 200 m of section. This excursion is developed over a thick stratigraphic interval in comparison to many sections documented to date. Elsewhere, the N1 excursion is typically expressed over tens of metres of section (Magaritz *et al.* 1986; Narbonne *et al.* 1994; Kaufman & Knoll 1995; Knoll *et al.* 1995*a*, *b*; Pelechaty *et al.* 1996*b*). The thick N1 shift of the Tinnaya Formation is interpreted to signify the lack of post-Vendian erosion, high subsidence rates in the basin, and conditions of high preservation potential in deep-water. In northeast Siberia, the N1 shift is partially preserved beneath the sub-Cambrian karst; it is variably eroded across the basin, and at some localities (e.g. Kharalaukh Mountains;

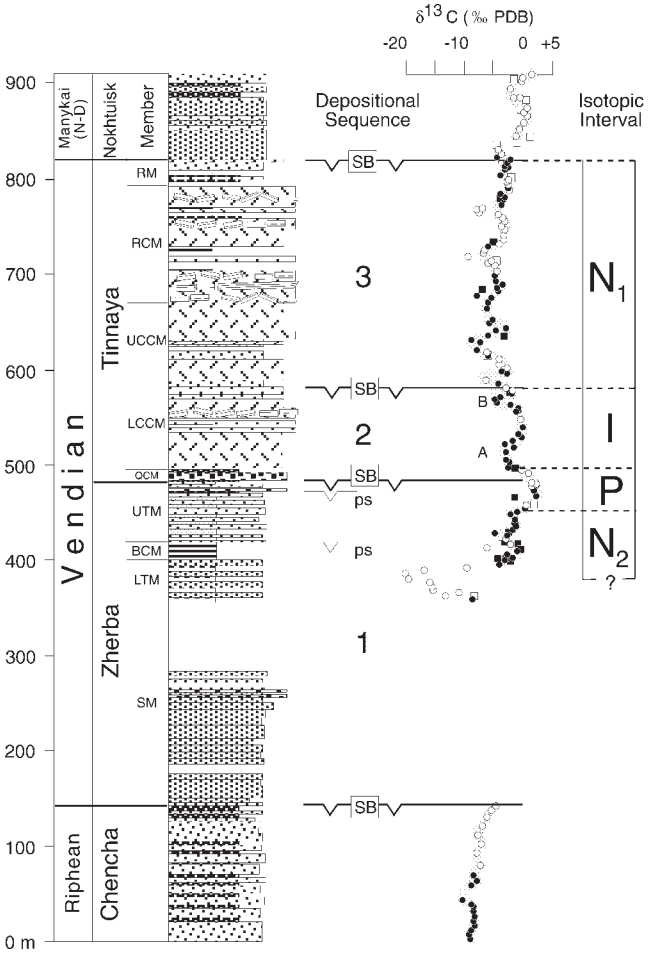

Fig. 7. Integrated sequence stratigraphic and carbon isotope chemostratigraphic framework for the Nokhtuisk section, showing the position of sequence boundaries (SB) and parasequences (ps), and major isotopic intervals, including a negative excursion (N2), a positive excursion (P), an intermediate interval (I), and an upper negative isotope anomaly (N1). Note the position of the interpreted Vendian-Cambrian boundary at the top of the Tinnaya Formation.

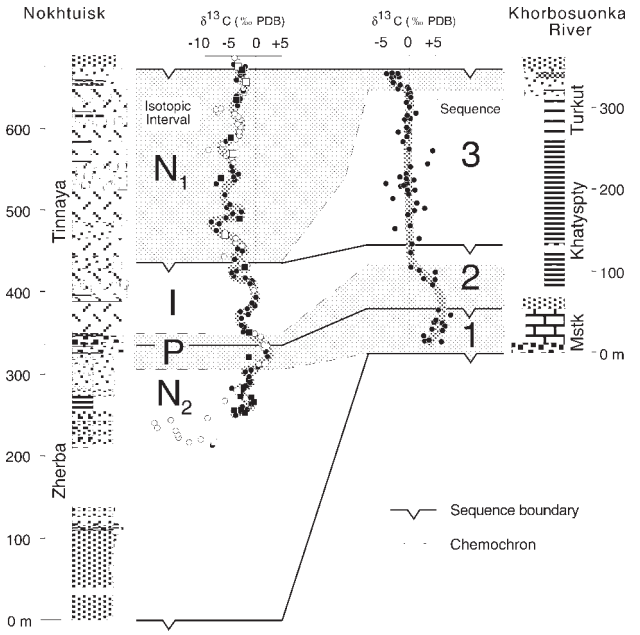

Fig. 8. Proposed chemo- and sequence stratigraphic correlation of the Nokhtuisk section and the Khorbosuonka River section in northern Siberia. The $\delta^{13}C$ profile and sequence stratigraphic framework for the Khorbosuonka River section are from Knoll *et al.* (1995*a*) and Pelechaty *et al.* (1996*b*), respectively.

Pelechaty *et al.* 1996*a*), the negative shift is completely eroded. In the south, however, a complete negative isotopic cycle is preserved, probably because of the limited amount of erosion that occurred during development of the sub-Nokhtuisk unconformity. Preservation of the isotopic signal in deep-water carbonates also implies the presence of limited stratigraphic breaks through the Tinnaya Formation, which probably favoured the preservation of a high-frequency signal characteristic of the N1 shift. Similar high-frequency signals are not observed in coeval shallow-water sections, and may not be expected in these sections, because of the high abundance of stratigraphic breaks inherent to shallow-water settings (e.g. Magaritz *et al.* 1986; Knoll *et al.* 1995*b*; Pelechaty *et al.* 1996*a*; Saylor 1996).

The relative thickness of the isotopic events of the Nokhtuisk profile also signifies subsidence history. The Nokhtuisk profile reveals a prominent N1 shift and relatively condensed I, P and N2 excursions. In comparison, the I interval is the most stratigraphically important isotopic event in many basins, including Namibia (Grotzinger *et al.* 1995), northwest Canada (Narbonne *et al.* 1994), and northeast Siberia (Knoll *et al.* 1995*a*; Pelechaty *et al.* 1996*a*). Nevertheless, the relative magnitude, shape and stratigraphic thickness of these isotopic events are seen to reflect basin subsidence history, and may not reflect temporal significance (Pelechaty *et al.* 1996*a*). The thick negative anomaly in the Tinnaya Formation most likely records relatively high rates of accommodation and sediment accumulation associated with few stratigraphic breaks in comparison to the compressed I and P intervals.

Chronostratigraphy of the Siberian platform

A single integrated chronostratigraphic framework is proposed herein for the Vendian System of eastern Siberia, despite the vast geographic separation of sections and regional variability in lithology, depositional facies, and tectonic setting. This chronostratigraphy is based on correlation of nine stratigraphic sections located throughout the eastern platform, and consists of at least three major cratonic sequences that are keyed into an idealized carbon isotope profile (Figs 8 and 9).

To establish the regional significance of the sequence stratigraphic and chemostratigraphic patterns, the Nokhtuisk section is compared with the Khorbosuonka River section in northeast Siberia. Sequences 1, 2, and 3 of the Zherba and Tinnaya formations are interpreted to correlate with an identical number of similarly named sequences along the Khorbosuonka River (Fig. 8; Pelechaty *et al.* 1996*b*). In the Olenek area of northeast Siberia, a Vendian age for the Khorbosuonka Group and correlative deposits in the nearby Kharaulakh Mountains is constrained by radiometric age dates and occurrences of Ediacaran fauna (Bowring *et al.* 1993; Knoll *et al.* 1995*a*). The Khorbosuonka River section displays the most complete carbon isotope record in the area with three isotopic events (e.g. P, I and N1), as well as three major depositional sequences (Pelechaty *et al.* 1996*b*). Sequence 1 includes the Mastakh Formation and, isotopically, is

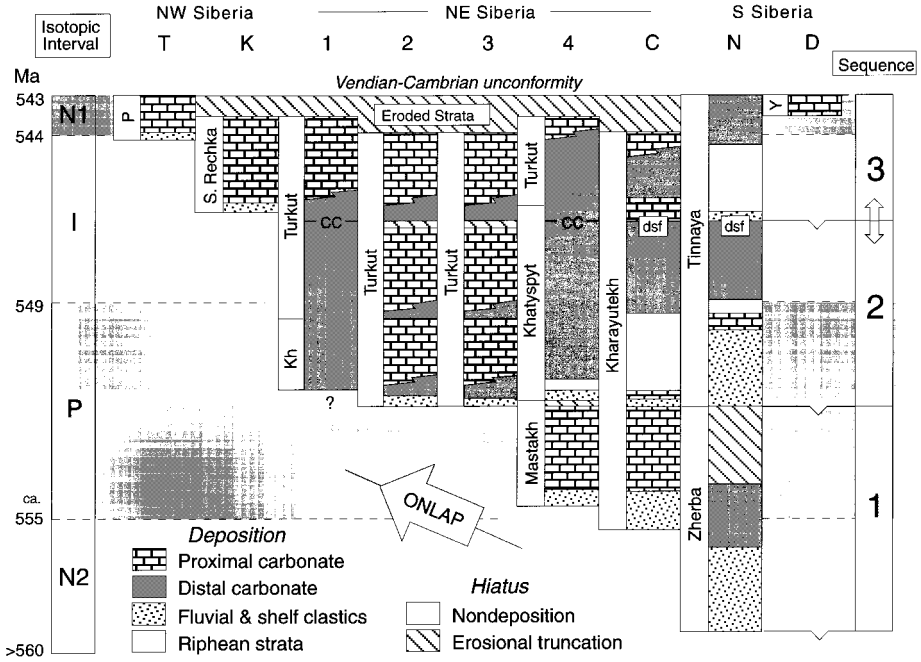

Fig. 9. Proposed integrated chronostratigraphic framework for the Vendian System of Siberia based on regional $\delta^{13}C$ chemo- and sequence stratigraphy. Location of sections is shown in Fig. 1. Stratigraphic sections: Turukhansk (T, Bartley *et al.* in press); Koutikhan River (K, Knoll *et al.* 1995*b*); Olenek uplift (1, 2, & 4, Pelechaty *et al.* 1996*b*; 3, Knoll *et al.* 1995*a*); Chukurov Anticline in the Kharaulakh Mountains (C, Pelechaty *et al.* 1996*b*); Nokhtuisk section (N, this study); and Dvortsy (D, Magaritz *et al.* 1986). Formations: Platonovka (P); Staraya (S) Rechka; Khatyspyt (Kh); Yudoma Series (Y). Abbreviations: correlative conformity (cc); downward shift in facies (dsf). Age constraints for idealized $\delta^{13}C$ profile are from radiometric age dates reported by Bowring *et al.* (1993) and Grotzinger *et al.* (1995), and estimated ages based on sediment compaction studies by Saylor (1996).

represented by the lower P interval; Sequence 2 in the lower part of the Khatyspyt Formation includes the upper P and lower I intervals; and Sequence 3, represented by the upper Khatyspyt and Turkut formations, includes the I and N1 intervals. The intra-Vendian sequence boundaries are positioned in the P (top of Sequence 1) and I (top of Sequence 2) intervals.

Regional correlation of Sequence 1 illustrates the diachroneity of basal Vendian strata in Siberia. Sequence 1 at the Khorbosuonka River section is thin and represents late-stage onlap onto the craton in comparison to the depositional record in the south, which began prior to 'N2 time' and is represented by a thicker depositional sequence. The P shift marks the top of the sequence at both localities and straddles the boundary between sequences 1 and 2. The P shift reaches values of +6‰ in the north but the same shift in the south is comparatively smaller with values less than +2.2‰. Evidence for several unconformities at this level in the Zherba Formation, however, strongly suggests that the present-day expression of this shift is an erosional remnant.

Sequence 2 at the Khorbosuonka River section is characterized by the upper P shift and the lower I interval. A similar signal but with added isotopic variability is interpreted to characterize the same sequence at the Nokhtuisk section. The slightly positive values at the base of the sequence are suggestive of the P shift, and the values near 0‰ through the middle of the sequence are representative of the I interval. A major discontinuity represented by a flooding surface at the base of the slope conglomerates may further account for the absence of a large positive excursion as observed at the Khorbosuonka section. In the north, however, the P shift is also missing in the outer basin sections (e.g. Kharalaukh Mountains); the P interval disappears into the basin as the result of downlap onto the sequence boundary (e.g. base of Sequence 2; Pelechaty *et al.* 1996*b*).

Additional isotopic variability is expressed in Sequence 2 in the south as two negative isotopic shifts (A and B, Fig. 7). The possible development of similar isotopic variability in other sections suggests that these anomalies may be secular in origin. For example, 2–4‰ negative shifts occur just above the P interval in carbonates of the Kuibis Formation in Namibia (Grotzinger *et al.* 1995; Saylor 1996), in the Turkut Formation on the west flank of the Olenek uplift (Fig. 9; Pelechaty *et al.* 1996*a*), and in the Staraya Rechka Formation in the western Anabar area of northwest Siberia (Knoll *et al.* 1995*b*). Similar negative shifts are also observed in Mongolia and China (Lambert *et al.* 1987; Brasier *et al.* 1996). Anomaly B at the top of the sequence may represent similar variability through the I interval, or mark the base of the N1 excursion. In either case, the top of Sequence 2 is shown to be diachronous between the Nokhtuisk and Khorbosuonka River sections.

Chemostratigraphic correlation of the two sections also highlights a time partitioning in Sequence 3 that is characterized by an early phase of deposition in the north during the I interval, and a younger phase of deposition in the south during N1 time (Fig. 8). Onset of late-stage deposition at the Nokhtuisk section follows a significant hiatus in deposition associated with marine flooding and downlap at the base of the sequence. The relatively prolonged period of deposition in the south represented by the N1 shift is attributed to relatively high subsidence and minimal post-Vendian erosion. In the north, post-Vendian erosion has removed younger segments of the Vendian isotopic record (Pelechaty *et al.* 1996*b*).

Correlation of the remaining sections in NE Siberia (Fig. 9) is produced by Pelechaty *et al* (1996*b*). Additional chronostratigraphic data from the Turukhansk uplift (Section T; Bartley *et al.* 1998), western Anabar (Section K; Knoll *et al.* 1995*b*) and Dvortsy (Section D; Magaritz *et al.* 1986) sections illustrate comparatively brief records of deposition at the close of Vendian (Sequence 3) time (Fig. 9). The record of deposition at these localities signals late-stage onlap and deposition over palaeohighlands of the Aldan and Anabar shields. Regional correlation also reveals a major unconformity at the top of Vendian successions across the eastern Siberian platform (Pelechaty *et al.* 1996*b*). Recognition of

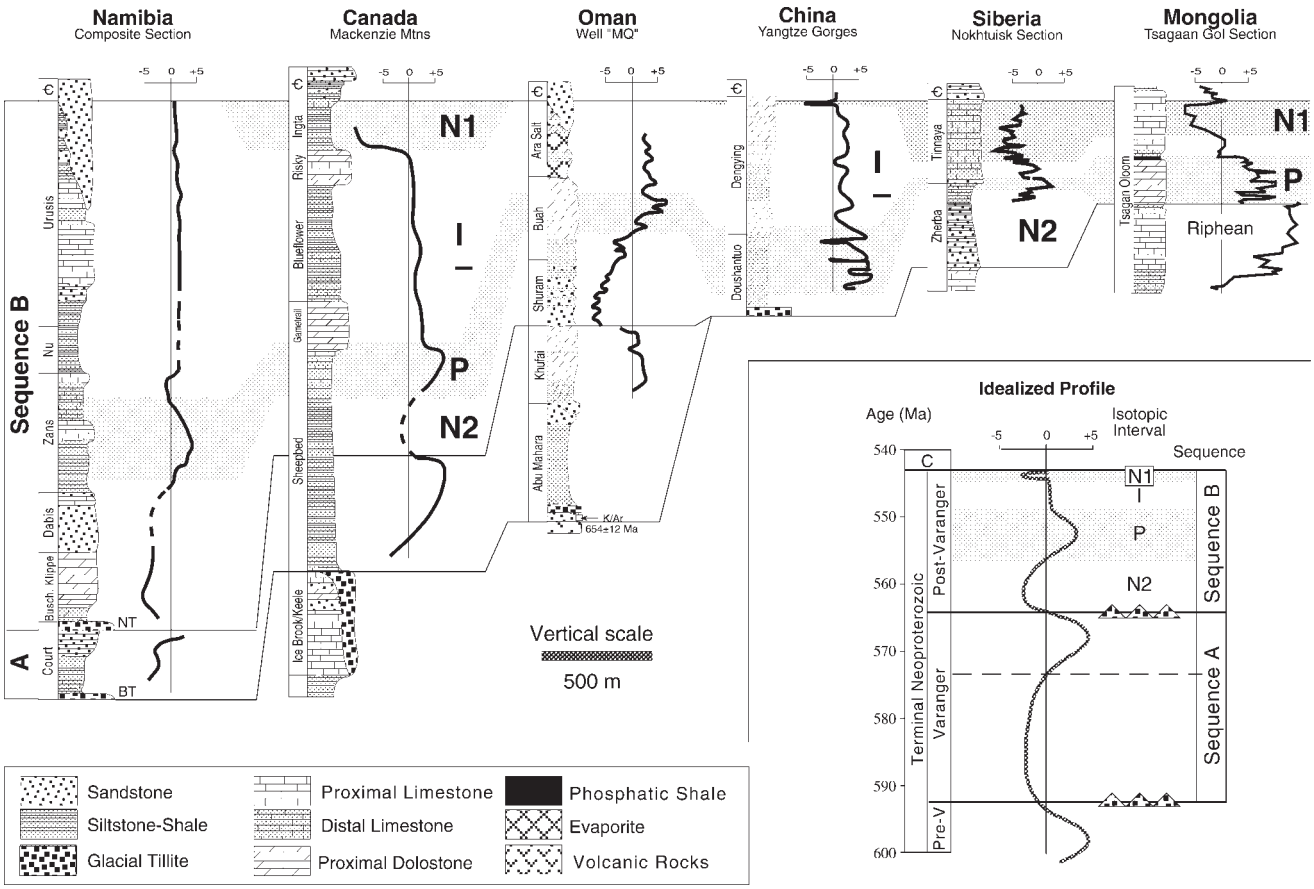

Fig. 10. Global correlation of key terminal Neoproterozoic sections based partially on chemostratigraphic correlation by Kaufman & Knoll (1995) and Saylor (1996), and a sequence stratigraphic framework herein proposed. Sections: northwest Canada (Narbonne *et al.* 1994); Namibia (Kaufman *et al.* 1991; Kaufman *et al.* 1993; Grotzinger *et al.* 1995; Saylor *et al.* 1995; Saylor 1996); Oman (Hughes Clarke 1988; Burns & Matter 1993); China (Lambert *et al.* 1987; Brookfield 1994); Siberia (this study); and Mongolia (Brasier *et al.* 1996). Namibian section: BT, Blaubeker tillite; NT, Naukluft tillite. SB, sequence boundary. Inset represents an ideal chronostratigraphy of carbon isotope excursions, sequence boundaries and distribution of tillites (modified from Saylor 1996; Saylor *et al.* in press).

unconformities at this level in a number of basins world-wide indicates a eustatic origin (Runnegar 1995), but pronounced erosion of strata in northern Siberia has been attributed to rift-related uplift coeval with a eustatic lowering of sea-level during separation of Siberia and Laurentia in the Early Cambrian (Pelechaty 1996; Pelechaty *et al.* 1996*b*).

The recognition of craton-wide sequences in Siberia suggests eustasy was a plausible mechanism for their formation. Radiometric age dates from Siberia and Namibia partially calibrate the Vendian carbon isotope profile (Bowring *et al.* 1993; Grotzinger *et al.* 1995), and suggest that the Siberian sequences represent third-order sea-level fluctuations. Nevertheless, correlation of these sequences on a global scale to test a eustatic hypothesis is difficult (e.g. Miall 1992), because of limited temporal control between basins. However, the Siberian sequences build a larger, second-order depositional sequence bounded by major unconformities that may be correlated globally with greater confidence using chemostratigraphic constraints. The second-order sequence includes the entire Vendian succession in eastern Siberia, and is represented by a lower assemblage of siliciclastic sediments and an upper assemblage of carbonates. Using available chemostratigraphy, coeval large-scale sequences are identified in other Neoproterozoic basins. Their global importance and the significance of the third-order sequences in Siberia are evaluated below.

Global correlation

Even though the Vendian stratigraphic record in Siberia is comparatively young, it exhibits major carbon isotope excursions that are documented in other basins in Namibia, Canada, Oman, China, Mongolia and elsewhere (Fig. 10; Lambert *et al.* 1987; Knoll & Walter 1992; Pell *et al.* 1993; Burns & Matter 1993; Narbonne *et al.* 1994; Kaufman & Knoll 1995; Grotzinger *et al.* 1995; Pelechaty *et al.* 1996*a*, *b*; Saylor 1996; Kaufman *et al.* 1997; Saylor *et al.* in press).

Combined chronostratigraphy (i.e. strontium and carbon isotope chemostratigraphy, geochronology, biostratigraphy and tillite stratigraphy) have enabled the development of a relatively high-resolution chronostratigraphic framework for terminal Neoproterozoic history (Bowring *et al.* 1993; Kaufman *et al.* 1993; Grotzinger *et al.* 1995; Kaufman & Knoll 1995; Saylor 1996; Kaufman *et al.* 1997; Saylor *et al.* in press). Multiple positive-to-negative carbon isotope excursions characterize terminal Neoproterozoic carbonates, and have been used to identify four to possibly five discrete glacial epochs (Saylor 1996; Kaufman *et al.* 1997; Saylor *et al.* in press). Saylor (1996) first suggested that the Varanger ice age probably does not represent a single glacial epoch, but instead includes several distinct glaciations of more local distribution, but recorded globally as changes in sea water chemistry. The

Varanger and post-Varanger time periods may be characterized by at least two major glaciations at 600 Ma and 565 Ma and associated with large-scale positive-to-negative carbon isotope excursions (see inset of Fig. 10). The older Varanger ice age is interpreted to be represented by the Blaubeker tillite in Namibia, the Ice Brook tillite in northwest Canada and tillites of the lower Abu Mahara Formation in Oman (Fig. 10; Saylor 1996; Kaufman *et al.* 1997). The younger, post-Varanger ice age includes the Naukluft tillite in Namibia, and glacial diamictites along the Yangtze Gorges in China. The apparent absence of latest Vendian age glacial deposits in Siberia may be explained by the equatorial position of the Siberian craton at this time, and its relatively young stratigraphic record.

In addition to identifying multiple tillites, global chemostratigraphic correlation of key sections also reveals an apparent second-order eustatic cyclicity, represented by at least two large-scale depositional sequences that appear to be closely associated with the distribution of tillites and carbon isotope excursions (Sequences A and B; inset of Fig. 10). These large-scale sequences are best developed in the Huqf Group in Oman, and in correlative deposits throughout the Middle East, Pakistan, and northern India (Fig. 10; Gorin *et al.* 1982; Hughes Clarke 1988; Husseini & Husseini 1990; Burns & Matter 1993; Burns *et al.* 1994; Peters *et al.* 1995). In general, the Huqf Group reveals an overall second-order packaging that is expressed by two major siliciclastic-to-carbonate trends bounded by major unconformities. In Oman, the oldest second-order sequence (Sequence A, Fig. 10) is interpreted to include deposits of the Abu Mahara and Khufai formations. Sequence A rests nonconformably on crystalline basement and includes tillites mixed with marine sandstones at its base, mixed sandstones and siltstones in the upper Abu Mahara Formation, and abruptly overlying these deposits, bituminous dolomites and then peritidal carbonates of the Khufai Formation. The top of Sequence A is marked by a karst erosion surface. Sequence B overlies the post-Khufai karst, and is represented as a siliciclastic–carbonate–evaporite package, including the Shuram, Buah, and Ara formations. The top of Sequence B is assigned to the unconformity at the base of the Haima sandstones. Other unconformities are also expressed in the Huqf Group but the unconformities bounding sequences A and B are highlighted for their apparent global significance. Others suggest an early Cambrian age for the Ara Formation (Mattes & Conway Morris 1990; Loosveld *et al.* 1996); however, several observations strongly suggest a late Vendian age for the Ara salt, including a carbon isotope chemostratigraphy resembling N2, P and I intervals, with the last event represented by invariant, positive $\delta^{13}C$ values through the Buah and Ara formations (Fig. 10; Burns & Matter 1993), and the presence of Ediacaran fauna in the Ara salt (see Kaufman & Knoll 1995). The unconformity capping the Ara salt at the base of the Cambrian age Haima sandstones is therefore interpreted to represent the Vendian–Cambrian boundary in Oman.

The deposits chemostratigraphically equivalent to Sequence A in Oman are present in Namibia and in northwest Canada (Fig. 10). The correlative sequence in Namibia is represented by the Court Formation. It is bounded by two tillite horizons and records lowering of sea-level (Fig. 10; Saylor 1996). The isotopically correlative strata in northwest Canada do not show an obvious drop in sea-level probably because of the relatively deep-water setting for this Canadian section, which contains a monotonous succession of deep-water siliciclastic deposits of the lower Sheepbed Formation above the Ice Brook tillite (Narbonne *et al.* 1994). Sequence B is represented in a greater number of basins world-wide and represents the onset of Vendian deposition in China, Siberia and Mongolia, as well as continued deposition in Namibia, Canada and Oman (Fig. 10). The Namibian section does not reveal an obvious transgressive-regressive pattern of sea-level change, which may reflect interference of local tectonically driven sea-level changes in the foreland basin (Saylor 1996).

The terminal Neoproterozoic record reveals multiple tillites and possibly second- and third-order (e.g. Siberia) eustatic sequences. Post-glacial transgression has been invoked to interpret records of sea-level rise recorded by sediments overlying tillites of pre-Nama Group strata in Namibia (Saylor 1996). However, glacioeustasy as a mechanism for the thicker, second-order depositional sequences is less obvious, because single deglaciations are difficult to invoke as the cause for major sea-level changes that occur over tens of millions of years. The importance of glacioeustasy at this time is difficult to assess, but may be greater than is now known. Saylor (1996) has asserted that, on the basis of evidence for additional tillite horizons in the upper Nama Group (Schwellnus 1942), and in the Lower Cambrian (Fersiga Group tillite) of northwest Africa (Bertrand-Sarfati *et al.* 1995), glacioeustasy was important throughout Sequence B time and into the early Cambrian. The glaciations have been suggested by Saylor (1996) to have occurred at 5 million year intervals. This cyclicity may have forced the third-order cratonic sequences in Siberia.

Phanerozoic first-order and second-order eustatic cycles record tectonoeustatic changes in sea-level related to variations in sea floor spreading during collision and breakup of continents (Pitman 1978; Bond *et al.* 1989; Hallam 1992). The significance of sea-floor spreading during terminal Neoproterozoic time is only speculative, because of the absence of oceanic crust to compare with the sea-level record. Nevertheless, the duration of the second-order sequences requires processes that operate over tens of millions of years, and thus sea-floor spreading provides a more plausible mechanism for the large-scale changes in eustatic sea-level, especially during the Neoproterozoic interval of wide spread continental breakup (Bond & Kominz 1984; Hoffman 1991; Moores 1991).

Initial transgression onto the Siberian platform during Vendian time has been viewed to have occurred well after Varanger deglaciation in northeast Siberia (Knoll *et al.* 1995*a*). Revised global correlation and new age constraints (Grotzinger *et al.* 1995; Saylor 1996) suggest that the base of older Vendian strata on the platform correlate with tillite horizons in China and Namibia (Fig. 10), and that flooding of the Siberian craton may have occurred in response to deglaciation. Higher in the stratigraphic section, early Cambrian transgression onto the Siberian craton may also correspond to a glacial epoch preserved in Africa (Bertrand-Sarfati *et al.* 1995); however, tectonic processes may equally well account for both Siberian transgressions. Fragmentation of Siberia and Laurentia in the early Cambrian may represent the final breakup of the supercontinent Rodinia (Pelechaty 1996, 1997*b*; Lieberman 1997). Geophysical models show that the insulating effects of supercontinents create a geoid high as the result of enhanced mantle convection (Gurnis 1988, 1990). The development of a pre-Cambrian geoid anomaly beneath the Siberian craton implies relatively limited subsidence and may explain the comparatively thin nature of the Vendian record in Siberia. Subsequent early Cambrian transgression onto the Siberian platform may reflect movement of the Siberian craton from such a geoid as the continent rifted from Laurentia at this

time. Increased sea floor spreading between the two cratons may have been an added mechanism for early Cambrian transgression on many continents (i.e. the base of the Sauk sequence of North America; Sloss 1963).

In summary, the latest Neoproterozoic record preserves evidence for global changes in sea water chemistry, multiple glaciations and eustatic changes in sea level at many scales, including high-frequency glacioeustasy and second-order sea-level change related to tectonoeustatic effects associated with breakup of the supercontinent Rodinia.

Conclusions

Integrated $\delta^{13}C$ chemostratigraphy and sequence stratigraphy yields a high-resolution time-stratigraphic framework for allochthonous Vendian deposits of southern Siberia. Vendian strata of the Zherba and Tinnaya formations display three major depositional sequences, and the carbonates exhibit secular variations in $\delta^{13}C$ with allowances for subsidence and breaks in the stratigraphic record. Correlation of this section with others on the Siberian platform reveals the development of three cratonic stratigraphic sequences. The sequences are most complete on the margins of the craton and less complete on the midcraton, because of influences of time transgressive onlap, limited accommodation and stratigraphic hiatuses.

Global correlation of the Vendian System of Siberia with other terminal Neoproterozoic successions provides evidence for eustasy by the recognition of correlative, second-order cycles in a number of sedimentary basins world-wide (i.e. Mongolia, China, Oman, Namibia, and Canada). At least two second-order cycles are recognized and form a physical stratigraphic context for the recognition of multiple tillites (Saylor 1996) and negative-to-positive $\delta^{13}C$ excursions from the start of Varanger glaciations at 600 Ma to the Precambrian–Cambrian boundary at 543 Ma (Saylor 1996; Kaufman *et al.* 1997). Evidence of repeated glaciations in Namibia possibly coeval with the Siberian cratonic sequences provides a plausible mechanism for these third-order sea-level changes. However, their influence on second-order sea-level oscillations is questionable; sea-floor spreading related to breakup of the supercontinent Rodinia provides a more plausible mechanism.

This research is part of my PhD dissertation at the Massachusetts Institute of Technology, under the supervision of J. P. Grotzinger. Financial support was provided by a Maxus Energy Fellowship, and logistical support for field work in Siberia was given by Yakutskgeofisica, Republic of Sakha. I especially thank V. Zhernovsky for his assistance during three field seasons in Siberia. This paper has benefited from discussions with S. A. Bowring, A. H. Knoll, P. H. Hoffman, and B. Z. Saylor. J. Southard and N. P. James are thanked for informally reviewing this manuscript. K. Lohmann is gratefully acknowledged for use of his laboratory at the University of Michigan. JGS reviewers G. Shields and H. Strauss are thanked for reviewing the paper.

References

ANDERSON, T.F. & ARTHUR, M.A. 1983. Stable isotopes of oxygen and carbon and their application to sedimentological and paleoenvironmental problems. *In*: ARTHUR, J.M.A. *et al.* (eds) *Stable Isotopes in Sedimentary Geology*. Society of Economic Paleontologists and Mineralogists, Short Courses, **10,** 1.1–1.151.

BARTLEY, J.J., POPE, M., KNOLL, A.H., SEMIKHATOV, M.A. & PETROV, P.YU. In press. A Vendian-Cambrian boundary succession from the northwestern margin of the Siberian Platform: Stratigraphy, palaeontology, chemostratigraphy, and correlation. *Geological Magazine,* **135,** 473–494.

BERTRAND-SARFATI, J., MOUSSINE-POUCHKINE, A., AMARD, B. & AIT KACI AHMAED, A. 1995. First Ediacaran fauna found in western Africa and evidence for an Early Cambrian glaciation. *Geology,* **23,** 133–136.

BOBROV, A.K. 1964. *Geology of the Predbaikal region: Structure and prospectivity of oil and gas.* Nauka [in Russian].

—— 1979. *Stratigraphy and paleogeography of deposits of the upper Precambrian of southern Yakutia.* Yakutian Book Publishing, Yakutsk [in Russian].

BOND, G.C. & KOMINZ, M.A. 1984. Construction of tectonic subsidence curves for the early Paleozoic miogeocline, southern Canadian Rocky Mountains: Implications for subsidence mechanisms, age of breakup, and crustal thinning. *Geological Society of America Bulletin,* **95,** 155–173.

——, ——, STECKLER, M.S. & GROTZINGER, J.P. 1989. Role of thermal subsidence, flexure, and eustasy in the evolution of early Paleozoic passive-margin carbonate platforms. *In*: CREVELLO *et al.* (eds) *Controls on Carbonate Platform and Basin Development*. Society of Economic Paleontologists and Mineralogists Special Publications, **44,** 39–61.

BOWRING, S.A., GROTZINGER, J.P., ISACHSEN, C.E., KNOLL, A.H., PELECHATY, S.M. & KOLOSOV, P. 1993. Calibrating rates of early Cambrian evolution. *Science,* **261,** 1293–1298.

BRASIER, M.D., SHEILDS, G., KULESHOV, V.N. & ZHEGALLO, E.A. 1996. Integrated chem- and biostratihgraphic calibration of early animal evolution: Neoproterozoic-early Cambrian of southwest Mongolia. *Geological Magazine,* **133,** 445–485.

BROOKFIELD, M.E. 1994. Problems in applying preservation, facies and sequence models to Sinian (Neoproterozoic) glacial sequences in Australia and Asia. *Precambrian Research,* **70,** 113–143.

BURNS, S.J. & MATTER, A. 1993. Carbon isotopic record of the latest Proterozoic from Oman. *Eclogae Geologicae Helvetiae,* **86,** 597–607.

——, HAUDENSCHILD, U. & MATTER, A. 1994. The strontium isotopic composition of carbonates from the late Precambrian (560–540 Ma) Huqf Group of Oman. *Chemical Geology,* **111,** 269–282.

CHOQUETTE, P.W. & JAMES, N.P. 1988. Introduction. *In*: JAMES, N.P. & CHOQUETTE, P.W. (eds) *Paleokarst*. Springer-Verlag, New York, 1–24.

CLAYPOOL, G.E. & THRELKELD, C.N. 1983. Anoxic diagenesis and methane generation in sediments of the Blake outer ridge DSDP 533, Leg 76. *Initial reports of the Deep Sea Drilling Project,* **76,** 391–402.

COOK, H.E. & MULLINS, H.T. 1983. Basin margin environment. *In*: SCHOLLE, P.A., *et al.* (eds) *Carbonate Depositional Environments.* American Association of Petroleum Geologists, Memoirs, **33,** 540–617.

—— & TAYLOR, M.E. 1977. Comparison of continental slope and shelf environments in the Upper Cambrian and Lowest Ordovician of Nevada. *In*: COOK, H.E. & ENOS, P. (eds) *Deep Water Carbonate Environments.* Society of Economic Paleontologists and Mineralogists, Special Publications **25,** 51–81.

ESTABAN, M. & KLAPPA, C.F. 1983. Subaerial Exposure. *In*: SCHOLLE, P.A., *et al.* (eds) *Carbonate Depositional Environments.* American Association of Petroleum Geologists, Memoirs, **33,** 1–93.

GORIN, G.E., RACZ, L.G. & WALTER, M.R. 1982. Late Precambrian-Cambrian sediments of Huqf Group, Sultanate of Oman. *American Association of Petroleum Geologists Bulletin,* **66,** 2609–2627.

GROSMAN, V.V. & ZHERNOVSKY, V.P. 1989. About upper Precambrian and Cambrian boundary strata in deep wells of western Yakutia. *In*: KHOMENTOVSKY, V.V., *et al.* (eds) *Late Precambrian and Early Paleozoic of Siberia: Actual Stratigraphic Questions.* Russian Academy of Sciences, Novosibirsk, 75–106 [in Russian].

GROTZINGER, J.P., BOWRING, S.A., SAYLOR, B.Z. & KAUFMAN, A.J. 1995. Biostratigraphic and geochronological constraints on early animal evolution. *Science,* **270,** 598–604.

GURNIS, M. 1988. Large scale mantle convection and the aggregation and dispersal of supercontinents. *Nature,* **332,** 695–699.

—— 1990. Plate-mantle coupling and continental flooding. *Geophysical Research Letters,* **17,** 623–626.

HALLAM, A. 1992. *Phanerozoic Sea-level Changes.* Columbia University Press, New York.

HISCOTT, R.N. & JAMES, N.P. 1984. Carbonate debris flows, Cow Head Group, western Newfoundland. *Journal of Sedimentary Petrology,* **55,** 735–745.

HOFFMAN, P.H. 1991. Did the breakout of Laurentia turn Gondwanaland inside out? *Science,* **252,** 1409–1413.

HUGHES CLARKE, M.W. 1988. Stratigraphy and rock unit nomenclature in the oil-producing area of interior Oman. *Journal of Petroleum Geology,* **11,** 5–60.

HUSSEINI, M.I. & HUSSEINI, S.I. 1990. Origin of the Infracambrian salt basins of the Middle East. *In*: BROOKS, J. (ed.) *Classic Petroleum Provinces.* Geological Society of London, Special Publications, **50,** 279–292.

JAMES, N.P. & STEVENS, R.K. 1986. Stratigraphy and correlation of the Cambro-Ordovician Cow Head Group, western Newfoundland. *Geological Survey of Canada, Bulletin,* **336,** 143

KAUFMAN, A.J. & KNOLL, A.H. 1995. Neoproterozoic variations in the C-isotopic composition of seawater: Stratigraphic and biogeochemical implications. *Precambrian Research,* **73,** 27–50.

——, HAYES, J.M., KNOLL, A.H. & GERMS, G.J.B. 1991. Isotopic compositions of carbonates and organic carbon from upper Proterozoic successions in Namibia: stratigraphic variation and the effects of diagenesis and metamorphism. *Precambrian Research,* **9,** 301–327.

——, JACOBSON, S.B. & KNOLL, A.H. 1993. The Vendian record of Sr and C isotopic variations in seawater: Implications for tectonics and paleoclimate. *Earth and Planetary Science Letters,* **120,** 409–430.

——, KNOLL, A.H. & NARBONNE, G.M. 1997. Isotopes, ice ages, and terminal Proterozoic earth history. *Proc. Natl. Acad. Sci. U.S.A.,* **94,** 6600–6605.

——, ——, SEMIKHATOV, M.A., GROTZINGER, J.P., JACOBSEN, S.B. & WILLIAM, A. 1996. Integrated chronostratigraphy of Proterozoic–Cambrian boundary beds in the western Anabar region, northern Siberia. *Geological Magazine,* **133,** 509–532.

KHOMENTOVSKY, V.V. 1986. The Vendian System of Siberia and a standard stratigraphic scale. *Geological Magazine,* **123,** 333–348.

—— 1990. Chapter 5: Vendian of the Siberian Platform. *In*: SOKOLOV, B.S. & FEDONKIN, M.A. (eds) *Vendian System.* Springer-Verlag, Berlin, **2,** 103–183.

KLEIN, G.D. 1977. *Clastic Tidal Flats.* COPCO, Champaign, Illinois, 149.

KNOLL, A.H. & WALTER, M.R. 1992. Latest Proterozoic stratigraphy and earth history. *Nature,* **356,** 673–678.

——, GROTZINGER, J.P., KAUFMAN, A.J. & KOLOSOV, P. 1995*a*. Integrated approaches to terminal Proterozoic stratigraphy: An example from the Olenek Uplift, northeastern Siberia. *Precambrian Research,* **73,** 251–270.

——, KAUFMAN, A.J., SEMIKHATOV, M.A., GROTZINGER, J.P. & ADAMS, W. 1995*b*. Sizing up the sub-Tommotian unconformity in Siberia. *Geology,* **23,** 1139–1143.

——, —— & —— 1995*c*. The carbon-isotopic composition of Proterozoic carbonates: Riphean successions from northwestern Siberia (Anabar massif, Turukhansk uplift). *American Journal of Science,* **295,** 823–850.

KOCURKO, M.J. 1986. Interaction of organic matter and crystallization of high magnesium calcite, south Lousianna. *In*: GAUTIER, D.L. (ed.) *Roles of Organic Matter in Sediment Diagenesis.* Society of Economic Paleontologists and Mineralogists, Special Publications, **38,** 13–21.

KOLOSOV, P.N. 1975. *Stratigraphy of upper Precambrian of southern Yakutia.* Nauka [in Russian].

KUZNETSOV, V.G. & SUCHY, V. 1992. Vendian–Cambrian tidal and sabkha facies of the Siberian platform. *Facies,* **27,** 285-294 [in Russian].

LAMBERT, I.B., WALTER, M.R., WENLONG, Z., SONGNIAN, L. & GUOGAN, M. 1987. Paleoenvironment and carbon isotope stratigraphy of Upper Proterozoic carbonates of the Yangtze Platform. *Nature,* **325,** 140–142.

LIEBERMAN, B. 1997. Early Cambrian paleogeography and tectonic history: A biogeographic approach. *Geology,* **25,** 1039–1042.

LOOSVELD, J.H., BELL, A. & TERKEN, J.J.M. 1996. The tectonic evolution of interior Oman. *GeoArabia,* **1,** 28–51.

MAGARITZ, M., HOSER, W.T. & KIRSCHVINK, J.L. 1986. Carbon-isotope events across the Precambrian-Cambrian boundary on the Siberian platform. *Nature,* **320,** 258–259.

MATTES, B.W. & CONWAY MORRIS, S. 1990. Carbonate/evaporite deposition in the late Precambrian-Early Cambrian Ara Formation of southern Oman. *In*: ROBERTSON, A.H.F., SEARLE, M.P. & RIES, A.C. (eds) *The Geology and Tectonics of the Oman Region.* Geological Society, London, Special Publications, **38,** 617–636.

MIALL, A.D. 1992. Exxon global cycle chart: An event for every occasion? *Geology,* **20,** 787–790.

MOORES, E.M. 1991. Southwest U.S.–East Antarctic (SWEAT) connection: A hypothesis. *Geology,* **19,** 425–428.

NARBONNE, G.M., KAUFMAN, A.J. & KNOLL, A.H. 1994. Integrated chemostratigraphy and biostratigraphy of the upper Windermere Supergroup (Neoproterozoic), Mackenzie Mountains, northwestern Canada. *Geological Society of America Bulletin,* **106,** 1281–1292.

NIKULIN, V.E. 1970. Main structures of the Baikal-Patom upland and adjacent areas. *In*: BOGOLEPOV, K.V. (ed.) *Tectonics of Siberia.* Nauka, Moscow, 35–39 [in Russian].

PELECHATY, S.M. 1996. Stratigraphic constraints for the Siberia-Laurentia connection and early Cambrian rifting. *Geology,* **24,** 719–722.

—— 1997*a*. *The Vendian–Cambrian System of Siberia: Correlation, Tectonics and Petroleum Geology*. PhD thesis, Massachusetts Institute of Technology.

—— 1997*b*. Stratigraphic constraints for the Siberia–Laurentia connection and early Cambrian rifting: Comments and Reply. *Geology,* **25,** 571–572.

——, GROTZINGER, J.P., KASHIRTSEV, V.A. & ZHERNOVSKY, V.P. 1996b. Chemostratigraphic and sequence stratigraphic constraints on Vendian-Cambrian basin dynamics, Northeast Siberian craton. *Journal of Geology,* **104,** 543–564.

——, KAUFMAN, A.J. & GROTZINGER, J.P. 1996a. Evaluation of $\delta^{13}C$ isotope stratigraphy for intrabasinal correlation: Vendian strata of the Olenek uplift and Kharaulakh Mountains, Siberian platform, Russia. *Geological Society of America Bulletin,* **108,** 992–1003.

PELL, S.D., MCKIRDY, D.M., JANSYN, J. & JENKINS, R.J.F. 1993. Ediacaran carbon isotope stratigraphy of South Australia—an initial study. *Royal Society of South Australia Transactions,* **117,** 153–161.

PETERS, K.E., CLARK, M.E., GUPTA, U.D., MCCAFFREY, M.A. & LEE, C.Y. 1995. Recognition of an Infracambrian source rock based on biomarkers in the Baghewala-1 oil, India. *American Association of Petroleum Geologists Bulletin,* **79,** 1481–1494.

PISCIOTTO, K.A. & MAHONEY, J.J. 1981. Isotopic survey of diagenetic carbonates, Deep Sea Drilling Project Leg 63. *In*: YEATS, R. S. & HAQ, B.U. (eds.) *Initial Reports Deep Sea Drilling Reports.* US Government Printing Office, Washington, **63,** 595–609.

PITMAN, W.C. 1978. Relationship between eustacy and stratigraphic sequences of passive margins. *Geological Society of America Bulletin,* **89,** 1389–1403.

POKROVSKY, B.G. & GERTSEV, D.O. 1993. Upper Precambrian carbonates with anomalously light carbon isotope composition (South-central Siberia). *Lithology and Mineral Resources,* **1,** 64–80 [in Russian].

—— & MISSARZHEVSKY, V.V. 1993. Isotopic correlation of Precambrian and Cambrian boundary beds of the Siberian platform. *Akademii Nauk Rossiya Doklady,* **329,** 768–771 [in Russian].

RUNNEGAR, B. 1995. Base of the Sauk sequence is a global eustatic event that lies just above the Precambrian-Cambrian boundary. *Geological Society of America, Abstracts with Programs,* **27,** A330.

SALTZMAN, M.R., DAVIDSON, J.P., HOLDEN, P., RUNNEGAR, B. & LOHMANN, K.C. 1995. Sea-level-driven changes in ocean chemistry at an Upper Cambrian extinction horizon. *Geology,* **23,** 893–896.

SAYLOR, B.Z. 1996. *Sequence stratigraphic and chemostratigraphic constraints on the evolution of the terminal Proterozoic to Cambrian Nama basin, Namibia.* PhD thesis, Massachusetts Institute of Technology.

——, GROTZINGER, J.P. & GERMS, G.J.B. 1995. Sequence stratigraphy and sedimentology of the Neoproterozoic Kuibus and Schwarzrand Subgroups (Nama Group), southwestern Namibia. *Precambrian Research,* **73,** 153–171.

——, KAUFMAN, A.J., GROTZINGER, J.P. & URBAN, F.E. In press. The partitioning of terminal Neoproterozoic time: Constraints from Namibia. *Journal of Sedimentary Research,*.

SCHWELLNUS, C.M. 1942. The Nama tillite in the Klein Kharas mountains, SW Africa. *Geological Society of South Africa Bulletin,* **12,** 19–33.

SHENFEL, V.Y. 1991. *Late Precambrian of the Siberian Platform.* Science Academy of USSR, Novosibirsk [in Russian].

—— & YAKSHIN, V.G. 1975. New information on the stratigraphy of Late Proterozoic depostis along the Tokko River basin: Analagous to the Siberian Vendian Complex. *Nauka,* 146–151 [in Russian].

SLOSS, L.L. 1963. Sequences in the cratonic interior of North America. *Geological Society of America Bulletin,* **74,** 193–214.

SOCHAVA, A.V., PODKOVYROV, V.N. & VINOGRADOV, D.P. 1996. Variations of carbon and oxygen isotope compositions in Vendian-Lower Cambrian carbonate rocks of the Ura Anticlinorium (southern Siberian platform). *Lithology and Mineral Resources,* **31,** 248–257.

VAIL, P.R., HARDENBOL, J. & TODD, R.G. 1984. Jurassic unconformities, chronostratigraphy, and sea-level changes from seismic stratigraphy and biostratigraphy. *In*: SCHLEE, J.S. (ed.) *Interregional Unconformities and Hydrocarbon Accumulations.* American Association of Petroleum Geologists, Memoirs, **36,** 129–144.

WEIMER, R.J., HOWARD, J.D. & LINDSAY, D.R. 1982. Tidal flats and associated tidal channels. *In*: SCHOLLE, P.A. & SPEARING, D. (eds) *Sandstone Depositional Environments.* International Association of Sedimentologists, Special Publications, **2,** 205–224.

Received 29 January 1997; revised typescript accepted 8 March 1998.
Scientific editing by Alistair Crame.